

**INFLUENCE OF VIBRATION AND STAGE
CONSTRUCTION ON THE PERCEPTION OF
MUSICAL PERFORMANCE**

By

Clemeth L. Abercrombie

A Thesis Submitted to the Graduate
Faculty of Rensselaer Polytechnic Institute

in Partial Fulfillment of the
Requirements for the Degree of

MASTER OF SCIENCE

Major Subject: BUILDING SCIENCES, ARCHITECTURAL ACOUSTICS

Approved:

Dr. Jonas Braasch, Thesis Adviser

Dr. Ning Xiang, Thesis Adviser

Rensselaer Polytechnic Institute
Troy, New York

June 2009
(For Graduation August 2009)

© Copyright 2009
by
Clemeth L. Abercrombie
All Rights Reserved

CONTENTS

LIST OF TABLES	v
LIST OF FIGURES	vii
ACKNOWLEDGMENT	xi
ABSTRACT	xii
1. Introduction	1
2. Motivation	3
2.1 Stage Acoustics	3
2.2 Multimodal Perception and Telepresence	4
2.3 Multimodal Perception and Whole-body Vibration	4
2.4 Multidimensional Scaling	7
3. Tactile Perception	9
3.1 Whole-body Vibration	9
3.1.1 Sensation Level	9
3.1.2 Frequency	12
3.1.3 Time	15
3.1.4 Other Factors	16
4. Structural Vibration	17
4.1 Theoretical Mechanics of Motion	17
4.2 Receptance, Mobility, and Accelerance	19
4.3 Measurements	20
5. Experimental Design	23
5.1 Data Collection	23
5.1.1 Musical Source Material	25
5.1.2 Stage Structural Response	26
5.2 Audio-Tactile Display	30
5.2.1 Motion Platform	30
5.2.2 Binaural Audio	33
5.3 Subjective Testing	34

5.3.1	Multidimensional Scaling	34
5.3.1.1	Definition	34
5.3.1.2	Application	37
5.3.2	Subjective Testing	40
6.	Results and Analysis	43
6.1	Structural Response	43
6.1.1	Magnitude	45
6.1.2	Frequency	47
6.1.3	Time	48
6.2	Human Response	50
6.2.1	Multidimensional Scaling Configurations	50
6.2.1.1	Two-Way MDS	50
6.2.1.2	Individual Difference Scaling	51
6.2.2	Correlation to Physical Parameters	53
6.2.3	Survey Responses	62
7.	Discussion	63
7.1	Structural Response	63
7.2	Human Response	65
8.	Summary and Conclusions	69
	LITERATURE CITED	71
	APPENDICES	
A.	Mathematical Symbols	75
B.	Confounding Factors in the Perception of Vibration	77
C.	Stage Construction Details and Structural Response Measurement Positions	79
D.	Institutional Review Board Approved Informed Consent Form	82
E.	Measurement Equipment Specifications	85
F.	Structural Response Magnitudes	89
G.	Structural Frequency Response Functions	90
H.	Vibration Propagation Times	95
I.	Individual Subject Difference Matrices	96

J. Correlation Coefficients for MDS Configuration Axis and Physical Parameters 101

LIST OF TABLES

3.1	Semantic labels associated with physical magnitudes of acceleration (adapted from <i>Handbook of Human Vibration</i> [18].)	11
3.2	Vibration experienced during common events (adapted from <i>Handbook of Human Vibration</i> [18].)	12
4.1	Definitions of frequency response functions used in structural modal analysis.	20
5.1	Sample difference matrix used in Multidimensional Scaling. Each cell represents the perceptual difference between the stimulus associated with row i and column j	35
5.2	Rules of thumb for evaluating Kruskal’s Stress-1 goodness-of-fit measure [8].	39
5.3	Stimuli used for Subjective Experimentation.	40
6.1	Difference matrix found by averaging subjective difference ratings across subjects.	51
6.2	Physical parameters measured at the middle of the seat with a 180-lb human subject seated on the platform. %>thresh. = % of signal above human threshold for perception, W_k = frequency weighting, B.R. = bass ratio, Spec. CoG = spectral center of gravity.	55
F.1	Vibration magnitudes measured in unweighted and W_k ms ⁻² weighted acceleration between 10 and 100 Hz. Values represent the response to a 1 Newton unit force impulse at each stage measurement position. . . .	89
H.1	Vibration propagation times between source and receiver and time delays of vibration signal with respect to audio calculated using the cross-correlation function. Negative time delays indicate tactile lead.	95
I.1	Difference matrix: Subject #1	96
I.2	Difference matrix: Subject #2	96
I.3	Difference matrix: Subject #3	97
I.4	Difference matrix: Subject #4	97
I.5	Difference matrix: Subject #5	98
I.6	Difference matrix: Subject #6	98

I.7	Difference matrix: Subject #7	99
I.8	Difference matrix: Subject #8	99
I.9	Difference matrix: Subject #9	100
I.10	Difference matrix: Subject #10	100
J.1	Pearson product-moment correlation coefficients for correlation of physical parameters to two-way MDS configurations.	102
J.2	Pearson product-moment correlation coefficients for correlation of physical parameters to individual difference scaling MDS configurations. . .	103

LIST OF FIGURES

3.1	Frequency axis used in evaluation of human vibration as defined in ISO 2631.	10
3.2	Frequency weighting curves defined in ISO 2631. The W_k curve corresponds to vibration in the vertical direction and the $W_{x,y}$ curves correspond to vibration in the horizontal direction.	13
3.3	Subjective frequency sensitivity as measured by Howarth and Griffin in comparison to standardized frequency weighting curves presented in BSI 6841 [20]. — Measured. BSI 6841 W_g is an asymptotic approximation to ISO 2631 W_k	14
4.1	a) Typical receptance frequency response function showing modal resonances. b) Detail of single resonant peak. Damping ratio is dependent upon the height and bandwidth of the peak. Taken from <i>Modal Testing: Theory and Practice</i>	21
4.2	Example mode shape. Acceleration is exaggerated for easy identification of nodes and antinodes.	22
5.1	Peak frequency weighted acceleration measured at 2 m on the Slab-A concrete slab stage construction during a musical contra bass performance. Absolute threshold of perception is approximately $0.01 \text{ ms}^{-2} W_k$	24
5.2	Diagram of musical source material recording system. Binaural audio is recorded with a Head Acoustics HMS V.II dummy head, the contrabass is isolated from influence of stage vibration by a spring/damper system and recorded with a PCB 333B50 accelerometer.	26
5.3	Structural response measurement locations. Dashes mark source positions, black circle marks receiver position.	27
5.4	Structural impulse response measurement equipment. Instrumented sledhammer used to measure force input, laser doppler vibrometer used to measure force output (isolated from stage with bungee cord). Not Shown: 150 lbs of sand placed on chair used to mass load receiver position, source position mass loaded by experimenter operating hammer.	28
5.5	Motion platform used in multimodal presentation of audio-tactile stimuli. Sennheiser HD280 headphones are used for audio presentation.	31

5.6	Frequency response measured at the bottom of hard wooden seat mounted to the motion platform before and after calibration. Measurements are made with a 180 lb human subject seated on the platform.	32
5.7	Computer interface used by subjects to operate experiment. Number values on the screen are controlled by a handheld video game controller.	42
6.1	Sample structural impulse response in the time domain measured at 2 m on the Slab-B construction in the sideways direction. Amplitudes are scaled so that their absolute maxima are equal.	43
6.2	Sample structural impulse response in the frequency domain measured at 2 m on the Slab-B construction in the sideways direction. Magnitude spectra represent the square amplitudes of force and acceleration.	44
6.3	Stage vibration response as a function of distance.	45
6.4	\log_{10} of stage vibration response as a function of distance. Individual measurements shown with linear regression lines.	46
6.5	Histogram of slopes observed in linear regression of logarithmic acceleration data plotted against distance.	47
6.6	Modal and non-modal accelerance frequency response functions typical of joisted and concrete slab stage constructions, respectively.	48
6.7	Vibration propagation times as a function of distance.	49
6.8	Time delay between vibration and audio signals as a function of distance.	50
6.9	Kruskal Stress-1 values calculated for two-way MDS configurations of five dimensionalities. “Random Data” represents Stress-1 values for an equivalent MDS configuration generated with a set of random numbers as the input.	52
6.10	Two-dimensional, two-way MDS configuration. Each point represents a different stimulus.	53
6.11	Kruskal Stress-1 values calculated for individual difference scaling MDS configurations of five dimensionalities. ‘Random Data’ represents Stress-1 values for an equivalent MDS configuration generated with a set of random numbers as the input.	54
6.12	Two-dimensional, individual difference scaling MDS configuration. Each point represents a different stimulus.	56
6.13	Two-dimensional subject space for individual difference scaling MDS configuration. Each vector represents a difference subject and the importance of each dimension used in making their difference ratings.	57

6.14	Coefficients of correlation between physical parameters and one-dimensional MDS configurations. 2 way configurations are shown by solid bars. 3 way configurations represent individual difference scaling models, and are shown in dashed bars.	58
6.15	Coefficients of correlation between physical parameters and two-dimensional MDS configurations. 2 way configurations are shown by solid bars. 3 way configurations represent individual difference scaling models, and are shown in dashed bars.	59
6.16	Coefficients of correlation between physical parameters and three-dimensional MDS configurations. 2 way configurations are shown by solid bars. 3 way configurations represent individual difference scaling models, and are shown in dashed bars.	60
6.17	Two-dimensional, two-way MDS configuration. Each point represents structural vibration perceived on a different stage construction. Stimuli are labeled with unweighted acceleration measured on the platform. . .	61
C.1	Stage Construction Slab-A.	79
C.2	Stage Construction Slab-B.	79
C.3	Stage Construction Joist-A.	80
C.4	Stage Construction Orchestra Pit Riser.	80
C.5	Stage Construction Joist-B.	81
G.1	Accelerance frequency response functions for Slab-A construction in the front direction.	90
G.2	Accelerance frequency response functions for Slab-A construction in the side direction.	91
G.3	Accelerance frequency response functions for Slab-B construction in the front direction.	91
G.4	Accelerance frequency response functions for Slab-B construction in the side direction.	92
G.5	Accelerance frequency response functions for Joist-A construction in the front direction.	92
G.6	Accelerance frequency response functions for Joist-A construction in the side direction.	93
G.7	Accelerance frequency response functions for Orchestra Pit Riser construction in the side direction.	93

G.8	Accelerance frequency response functions for Joist-B construction in the front direction.	94
G.9	Accelerance frequency response functions for Joist-B construction in the side direction.	94

ACKNOWLEDGMENT

As always, the first expression of gratitude is for my family and especially my parents C. F. and Lila Abercrombie. They have provided the unending inspiration and support upon which all my achievements are founded. I would also like to thank Angela Biagi, whose love and support have been particularly integral to the completion of this degree and thesis.

Professors Ning Xiang and Jonas Braasch have developed a fantastic program that will surely continue to develop and become a cornerstone of education in Architectural Acoustics. I thank them both for the many valuable lessons learned and their abundant interest in my and my fellow students' educations. Their most important lessons are to explore the boundaries of conventional wisdom and always question what may be possible.

Many others contributed to this research. I would like to thank all of my classmates in the Architectural Acoustics program at RPI for their numerous points of view and friendly competition—the best of luck to all of you. Bill Bergman provided guidance in craftsmanship, design of the motion platform and a friendly ear throughout the research. Michael Bullock kindly and skillfully performed the music used in subjective testing. Jens Blauert, Ian Hoffman and Todd Brooks all provided invaluable insight and time in their discussions of direction for this research. Finally, I would like to thank the authors of all papers cited in this study for their dedication to acoustics and their contributions to the never-ending search for new information.

ABSTRACT

The constant pursuit of new architectural design methods and expanding use of multi-sensory music presentation calls for increased knowledge of human response to audio-tactile stimuli. This thesis presents an experiment to explore the human ability to distinguish differences in tactile signals generated by musical sources coupled with typical stage floor constructions. A contrabass is used to generate binaural audio and vibration signals. The mechanical impedance of several stage constructions is measured and used to synthesize tactile signals generated when coupled to the contrabass. The audio and tactile signals are reproduced using headphones and a calibrated motion platform. Test participants are asked to identify differences in tactile signals given a fixed audio environment. Multidimensional scaling is used to identify perceptual dimensions in subjective responses. Results show that stage vibration exceeds the threshold of perception ranging with acceleration up to $0.04 \text{ ms}^{-2} W_k$ peak on one construction. Vibration attenuation, propagation times and modal damping vary with construction type and direction of propagation with respect to beams and joists. Sensation level dominates perceived differences between tactile signals, while audio-tactile time delays of up to 74 ms have little to no influence on perceptual differences.

1. Introduction

The information presented to humans about their environment by vibration is thought to be insignificant in comparison to that provided by sight and sound, and thus tactile stimulation is often ignored unless it causes a disturbance. One might not realize the levels of vibration that are generated in his environment until he has been asked to evaluate such signals. However, when vibration does exist we cannot ignore its influence on our perception of a situation. Imagine sitting in an airplane in flight and hearing the roar of the engines and moving air without the shaking of the seat and jumps of turbulence. Imagine hearing and seeing a rock concert, but not perceiving the impact of the kick drum and bass guitar. It is hard to understand the importance of the tactile mode of perception, until it is taken away.

Multimodal research, the study of how different modes or senses of human perception interact, allows us to explore perception by one mode in the presence of the others. While technically demanding, this type of research moves closer to evaluating human perception in its most natural form, with all types of input interacting. Audio and vision are the modes most often studied due to their importance in the exchange of information. When the interest moves beyond the exchange of information into the ability to communicate *presence*, the tactile, olfactory and gestation senses become important.

The performance of music in an ensemble is a complex and demanding task, and musicians make use of every method of communication possible. Audition is obviously important, but musicians also use eye contact, body language and reportedly the tactile sensation generated by instruments around them to communicate during a performance. Interest in the last form of communication, vibration, is witnessed by a growing interest in research of tactile music perception and the design of orchestral stage platforms.

This thesis marks a continuation and convergence of research in musician communication, the human perception of vibration, structural mechanics and virtual multimodal displays. Several general questions guide the current exploration:

- How important is structural vibration in the perception of a musical performance?
- How do the materials and technique by which a stage is constructed affect structural vibration generated by musical performance?
- How do humans differentiate tactile signals?
- What physical characteristics of musical vibration in structures control human perception?
- What requirements must be met to accurately represent the tactile mode of perception in a virtual display?

These questions and more discovered along the way are the motivation for conducting this study. An experiment outlined in Section 5 is designed to measure stage vibration generated by musical performances and human response to this vibration. A review of work conducted in the past is presented in Section 2 followed by highlights and useful information regarding tactile perception and structural mechanics in Sections 3 and 4. Results and methods of analysis are presented in Section 6 and their implications discussed in Section 7. Some answers to the questions above and other interesting findings are summarized in Section 8. A list of mathematical symbols and definitions used in this document can be found in Appendix A.

2. Motivation

The multidisciplinary approach to this study is inspired by the meeting of several different paths of research. These paths could be broadly categorized as stage acoustics, multimodal perception of vibration, telepresence research and multivariate statistical methods.

2.1 Stage Acoustics

Stage acoustics is a subfield of architectural acoustics concerned with the evaluation and design of the aural conditions experienced by musicians. Primary concerns include ability of musicians to communicate effectively and their overall comfort in performance. Documented study of musicians' subjective response to stage acoustics began in 1978 with a study by Marshall *et al.* and their finding that acoustic reflections within an early temporal window improve ensemble during performance [26]. Michael Barron provided controlled experimental data to show the importance of early reflections [4]. The results of early experiments in stage acoustics was continued and solidified by the development of three acoustical parameters used to quantify "stage support"—ST₁, ST₂ and ST_{late} [13], [14], later revised to ST_{early}, ST_{late}, and ST_{total} [15]. Research into the subjective preference of stage acoustics as a function of instrument type continues to be a hot topic [36], [34].

In addition to their focus on time-energy ratios, Marshall *et al.*, Barron and Gade acknowledged that the perception of stage acoustics is a multidimensional phenomenon influenced not only by the level, arrival time, timbre, and location of sound; but the instrument played and inter-subject differences in preference. The authors also note that some variation in subjective responses appear to be controlled by factors other than those under consideration. The presence of other factors in stage support for musicians raises the question as to the importance of other modes of perception in musicians' judgment of stage acoustics. A study of the interaction of perceptual modes such as vibration and sound will provide a broader perspective and help to more fully understand stage acoustics.

2.2 Multimodal Perception and Telepresence

Multimodal perception is the process of gathering information from all the human senses and the combining it into a coherent “image” of the world. The study of multimodal perception is of obvious interest in the understanding of how humans process complex, real world situations. The topic is frequently mentioned in unimodal studies, only to identify the presence of other factors affecting the results. Conducting a study in which all modes of perception are stimulated simultaneously is a difficult task. However, studies in which musical signals are presented to two or three modes simultaneously are currently being conducted in the fields of psychophysics and telepresence [9]. The impact and significance of non-auditory factors in acoustic presentation are summarized by Durand R. Begault [5].

2.3 Multimodal Perception and Whole-body Vibration

The focus of the current study is on the perception of vibration generated by musical sources in the presence of audio. While much of the research in human perception of vibration has been conducted in the interest of comfort or communication, as presented in Michael Griffin’s book *The Handbook of Human Vibration* [18], there has been a recent emergence of research in the perception of musical signals by authors such as Michael Daub, M. Ercan Altinsoy and Kent Walker, William Martens, and Sungyoung Kim [10],[23]. In musical situations, the type of vibration that is most often considered is *whole-body vibration* (see section 3.1).

These recent studies mark the first published investigations into the importance of vibration in the perception of musical performances and also happen to be multimodal. This is not surprising, as removing audio from a musical environment would drastically alter the perception. The three studies also share a common theme, focusing on the ability of humans to perceive time differences between audio and haptic musical source stimuli.

The study presented by Daub and Altinsoy is a short experiment to assess the human ability to perceive audio-tactile synchrony. In their study, audio and tactile signals were measured using a binaural microphone (dummy head) and seat-mounted accelerometer during the performance of a pipe organ in a church and a

cello supported by a board in an anechoic chamber. The signals were presented to listeners in unmodified form via headphones and a shaker chair except for inserting several time delays to both audio and tactile signals. The listeners were asked to identify the signals as “synchronous” or “asynchronous” in a two alternative forced choice test. There is no mention of frequency or level calibration for either the audio or tactile reproduction systems. The magnitudes of signals recorded were not calibrated.

Psychoacoustic test results indicated that the mean user identified the *point of subjective simultaneity* (PSS) at a -135 ms tactile delay (negative values indicating a tactile lead) for the pipe organ signal and a -29 ms tactile delay for the cello (subjects with musical experience choosing a -43 to -66 ms PSS). The authors note that a simple cross correlation between the signals in the time domain indicated that the audio and tactile organ stimuli were most similar when the tactile signals was moved forward by 119 ms (-119 ms delay with respect to audio), indicating that the tactile signal arrived later than the audio signal in the measurement. The cello signals were found to have the highest correlation at a -59 ms delay with respect to audio.

Daub and Altinsoy then draw the conclusion that the PPS was not equal to the *point of objective simultaneity* (POS) and that as a result, the measurement of tactile signals is not required for realistic audio-tactile reproduction. However, the experimental data seems to present an alternative hypothesis. The POS chosen by the authors is the point of 0 ms time delay between audio and tactile signals in the recording, leading to large error between the PSS and POS. If the POS is chosen to be the time at which the signals are most similar (measured using the cross correlation function), the POS and PSS selected by the subjects become much closer. With the POS at the time of maximum correlation, the subjective PSS would be a 16 ms tactile lead for the organ and 5 ms tactile for the cello (average of musical listeners). Finally, the authors’ conclusion that tactile signals are not necessary for accurate reproduction based on unequal POS and PSS ignores any information about magnitude and frequency contained in structural vibration.

Walker *et al.* presented a study to the Audio Engineering Society with a similar objective: to evaluate the human ability to identify time synchrony in audio-tactile signals produced by musical instruments. In this study, a surround sound microphone technique is used to record the performance of a kick drum, piano, pipe organ, and contrabass. Tactile signals were created from a combination of near-field microphone and contact pickup audio transducers and low pass filtered at 60 Hz. The signals were reproduced using a multi-channel loudspeaker system including a subwoofer and a wooden shaker platform measuring 2.4 m by 1.2 m. Subjects were seated in soft cushioned chairs. In this study, the authors acknowledge and attempt to record large structural resonances in the platform affecting the frequency content of the tactile signals presented. Calibration of level is accomplished only by a rough perceptual judgment of matched psychophysical sensation level between audio and tactile signals while seated on the chair. The authors indicate peak acceleration values recorded on the platform range from 0.98 ms^{-2} to 1.93 ms^{-2} , values exceeding those experienced during a rough car ride as reported by Griffin [18]. The POS chosen by Walker *et al.* is based on the synchronized recording and corrected for a time difference between the audio and tactile components of the reproduction system. As a result, the physical POS selected includes the difference in arrival time between the tactile signal measured *near* or *in contact* with the source and the audio signal traveling to the acoustic center of the microphone array.

Two experiments are conducted, the first to measure the PSS using a time-order judgment in which subjects are asked to identify which signal comes first—audio or tactile. The second experiment assesses the ability to perceive time synchrony by using a three interval two alternative forced choice task with time adjustments centered around the PSS measured in the time-order judgment task. Walker *et al.* come to similar conclusions as Daub and Altinsoy, with different instruments providing different tactile time delay values for the PSS. Overall, the values obtained by Walker *et al.* are much lower with the PSS/POS difference ranging from a -30.2 ms to 14.8 ms tactile delay with respect to audio, depending on instrument. In fact, these values are in the range of the POS/PSS differences in the Daub/Altinsoy study if the PSS were to be chosen using the point of maximum cross correlation.

Walker *et al.* go on to report that frequency content and temporal characteristics of the performance (legato or pizzicato playing styles) influence both the ability to perceived time-order and the resulting PSS. In addition, statistically significant inter-subject differences in time-order judgments are observed.

A review of the two recent studies indicates some confusion about the point of objective simultaneity in audio-tactile signals observed in real life conditions. In addition, the authors discuss a need for further study regarding the importance and human response to magnitude and frequencies differences occurring in structural vibration generated by musical sources. The current study addresses these areas of research.

2.4 Multidimensional Scaling

Multidimension scaling is a multivariate technique for the exploration of the structure of differences in a data set. It is most commonly used in perceptual experimentation to present stimuli in their natural form and discover the “dimensions” of perceived differences (see Section 5.3.1 for a full description). Multidimensional scaling, or MDS, was used by John Grey in his study on musical timbre presented in the *Journal of the Acoustical Society of American* in 1977 [16]. In his study, Grey presented subjects with musical tones synthesized to represent the natural differences in harmonic and temporal structure between musical instruments. Multidimensional scaling was used to identify perceptual dimensions governing the subjects’ ratings of differences in the musical tones. The perceptual dimensions were able to be linked to attributes of timbre such as “spectral energy distribution”, “spectral fluctuation” and “low amplitude, high-frequency energy in attacks.”

Multivariate techniques have also been applied to the study of perception in room acoustics by Kiminori Yamaguchi in 1972 and Schroeder, Gottlob and Siebrasse in 1974 [35], [32]. In these studies, subjects are presented with musical stimuli representing the sound field experienced at different locations in a concert hall. Both studies made use of a controlled sound source and measurements conducted in real halls in an attempt to present stimuli in the most natural manner possible at the time. Subjects are asked to rate differences in signals in Yamaguchi’s

study and preference in Schroeder *et al.*'s study. Multivariate techniques allowed the experimenters to extract important information about what physical attributes control perception in complex sound fields (MDS for Yamaguchi, principal component analysis for Schroeder *et al.*).

Presentation of signals in their natural form is an important benefit in early studies of perception in complex situations. The precedent set by these studies leads to the selection of a multivariate technique in this study of multimodal perception in audio and vibration. Many of the decisions made with respect to experimental design and analysis of results are influenced by the studies of Grey, Yamaguchi and Schroeder *et al.*

3. Tactile Perception

By nature, multimodal research requires a broad, multidisciplinary approach. Knowledge of structural vibration, wave propagation, modal measurement techniques, signal processing, auditory perception, tactile perception and cognition are all required to make sound decisions in experimental design and analysis of the audio-tactile human response. Information presented in the next two sections will provide an overview of some of the knowledge base required for experimentation and evaluation of results.

3.1 Whole-body Vibration

Whole-body vibration refers to vibratory excitation of the entire body by the supporting surface such as a floor or chair, as apposed to single point or small area excitation generated by sources such as the Braille system or a foot massager. Vibration is experienced by most individuals on a daily basis in transportation such as automobiles or trains and structural vibration occurring in architecture generated by footfall or building service equipment such as large fans or compressors. As a result, most of the research regarding the perception of whole-body vibration has been conducted in search of a means to quantify and evaluate the degree to which a certain vibration signal will cause discomfort or annoyance. However, the basic principles of level, time and frequency discrimination apply to the perception of any signal type. In this section, an introduction to the basic means of vibration perception will be presented.

3.1.1 Sensation Level

“Sensation level” is the perceived intensity of vibration that is linked to physical measures of vibration amplitude such as acceleration or velocity. It is analogous to the perceived “loudness” of sound. As one might expect, the human response to vibration changes depending on how the body is supported and the direction(s) the supporting surface is moving. Several standards including ISO 2631 [2] have adopted

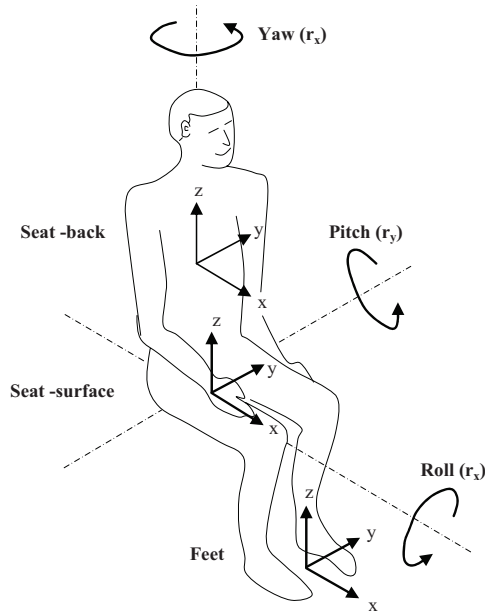


Figure 3.1: Frequency axis used in evaluation of human vibration as defined in ISO 2631.

a standard basicentric coordinate system with which to refer to the placement and direction of whole-body vibration shown in Figure 3.1. A single axis of vibration is often isolated in psychophysical experiments.

One of the first attributes of the tactile perception system studied is the absolute threshold of perception. Results of many these studies are presented in Griffin's handbook and have resulted in a generally accepted minimum physical magnitude of 0.01 ms^{-2} peak amplitude to be perceived by the average human exhibiting normal perception. Other levels of instantaneous vibration and corresponding semantic labels are presented in Table 3.1. Vibration magnitudes experienced in common events are listed in Table 3.2. Both tables are adapted from Griffin's handbook [18].

The standard method of evaluating the relationship between physical magnitude and psychophysical intensity is to use Steven's power law [18]. This relationship, presented in Equation 3.1, suggests that sensation level ψ will increase with physical magnitude ϑ according a constant growth exponent n where k depends on the units:

$$\psi = k\vartheta^n. \quad (3.1)$$

The growth exponent n will vary with axis of excitation, frequency, duration, and physical magnitude; but is expected to approach a mean value across subjects. Many studies have reported values of the growth exponent measured under various conditions, and are summarized in Griffin's Handbook [18]. Of particular interest in this study is a paper published by Howarth and Griffin in which the frequency dependence of sensation level is studied for signals at low amplitudes [20]. The authors report growth exponents between 1.04 to 1.47 for vertical (z-axis) motion and 0.68 to 1.99 for horizontal (y- and x-axis) motion for sine wave signals between 4 and 63 Hz presented at 6 magnitudes ranging from 0.04 to 0.4 ms^{-2} . The mean growth exponent value measured in the vertical direction is 1.2 and is statistically independent of frequency, while the mean value in the horizontal direction is 1.4 but varies with frequency.

Table 3.1: Semantic labels associated with physical magnitudes of acceleration (adapted from *Handbook of Human Vibration* [18].)

Semantic Label	$\text{ms}^{-2} W_k$ r.m.s.
Very strong perception	0.315
	0.25
	0.20
	0.16
Strong perception	0.125
	0.10
	0.08
Very clear perception	0.063
	0.05
	0.04
Clear perception	0.0315
	0.025
	0.02
Perception probable	0.016
	0.0125
	0.01
Perception improbable	0.008
	0.0063
	0.005

Table 3.2: Vibration experienced during common events (adapted from *Handbook of Human Vibration* [18]).

Vibration Type	Physical Magnitude
Smooth car ride	$0.2 \text{ ms}^{-2} W_k$ r.m.s.
Rought car ride	$1.0 \text{ ms}^{-2} W_k$ r.m.s.
Building vibration	$< 0.1 \text{ ms}^{-2} W_k$ r.m.s. $< 1.0 \text{ ms}^{-2} W_k$ peak

The results presented by Howarth and Griffin confirm the accepted estimate of a growth exponent of approximately 1—indicating a *linear* relationship between physical magnitude and sensation level [18],[20].

Morioka and Griffin have studied the "just noticeable difference" threshold, defined as the minimum physical magnitude by which a signal must be changed to result in a perceived difference [29]. The authors report that the human response follows the concept of Weber's fraction developed by German psychologist E. H. Weber shown in Equation 3.2 in which I represents perceived sensation level. The just noticeable difference in whole-body vibration is reported as approximately 10 % for sinusoidal signals at 5 and 20 Hz in the region of 0.1 and 0.5 ms^{-2} r.m.s.:

$$\frac{\Delta I}{I} = \text{constant.} \quad (3.2)$$

3.1.2 Frequency

Humans perceive vibrations of different frequencies to have different associated levels of sensation. This phenomena indicates that the human response to vibration is frequency dependent. One method of exploring this frequency dependence is to present sinusoidal or narrow band vibration signals to listeners and ask them to assign a subjective sensation level estimation based on a given reference signal and number, as conducted by Howarth and Griffin [20]. A second method is to present the same signals, but to adjust physical magnitudes of test stimuli until their test subjects indicate sensation levels match a target reference, as conducted by Mansfield and Maeda [25]. Results of these studies are often referred to as "equal sensation curves" or "equal sensation contours".

Significant variation in measured equal sensation curves has been presented, primarily due to the expected differences found when using test stimuli of different magnitude, frequency range and duration level [18]. In addition, differences in experimental conditions such as platform distortion, background noise and seat dynamics have also contributed to variation. Despite variation, the broad knowledge base has resulted in several standard frequency weightings, the most popular of which are presented International Organization for Standardization ISO 2631 and British Standards Institute BS 6841 [2], [3], [1]. The frequency weighting curve presented in Figure 3.2 has been designed for use in measuring the energy in a raw vibration waveform while adjusting frequencies to match equal sensation contours. As a result, the frequency weighted magnitude can be used to compare the expected sensation level generated by signals of different frequency. The general trends in this contour are marked by band limiting between 0.4 Hz and 100 Hz, a peak in sensitivity between 3 Hz and 12 Hz, and a steady decline in sensitivity between 12 Hz and 100 Hz that occurs as a result of the human response's correlation to velocity instead of acceleration.

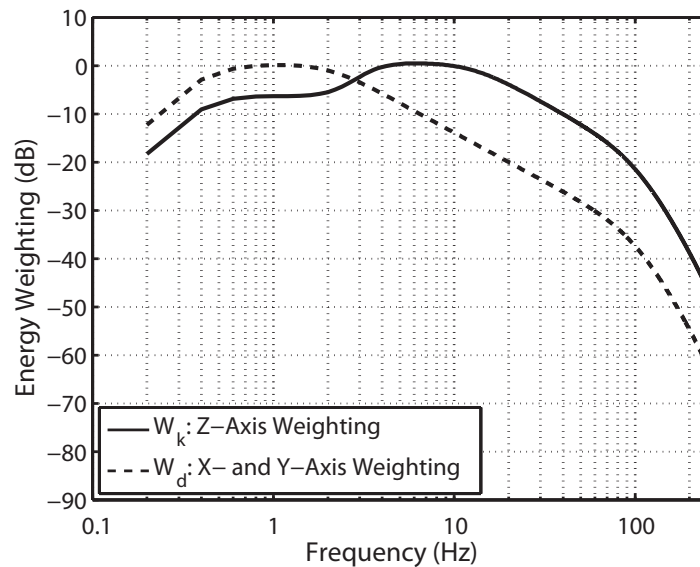


Figure 3.2: Frequency weighting curves defined in ISO 2631. The W_k curve corresponds to vibration in the vertical direction and the $W_{x,y}$ curves correspond to vibration in the horizontal direction.

Results of the study conducted by Howarth and Griffin using stimuli in the same frequency and amplitude range as those observed during musical performances on stage are in slight disagreement with the ISO 2631 frequency weighting curve, as shown in Figure 3.3. Their results shows that humans may be more sensitive to high frequencies at low magnitudes than indicated by the vertical frequency weighting curve W_k , which was created taking into consideration results of sensitivities measured across a wide range of experimental conditions.

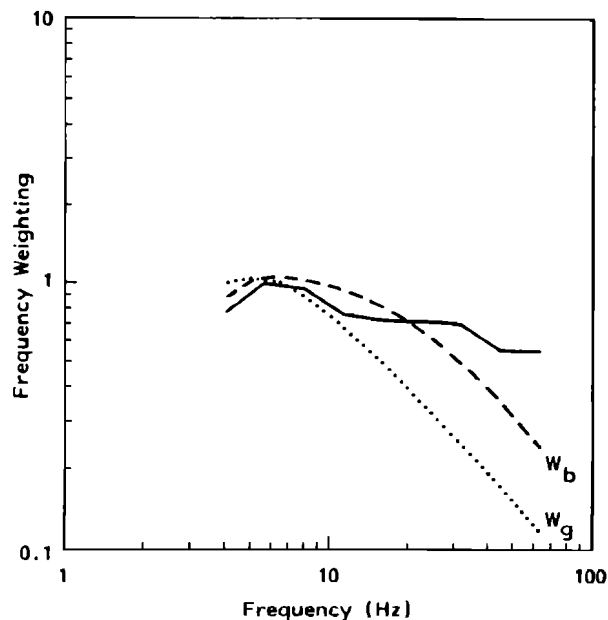


Figure 3.3: Subjective frequency sensitivity as measured by Howarth and Griffin in comparison to standardized frequency weighting curves presented in BSI 6841 [20]. — Measured. BSI 6841 W_g is an asymptotic approximation to ISO 2631 W_k .

A common theme in all equal sensation contours is a fairly broad smooth transition between frequencies. One explanation for the smoothness is the relatively few frequency data points obtained during experimentation. In addition, discussion presented by Griffin cites current research in biodynamics showing that high levels of damping and complex connections in the human body create a system in which no individual resonances dominate, leading to fairly smooth response across all frequencies of excitation for whole-body vibration [18]. Individual parts of the

body still possess resonant frequencies which can lead to different areas of localized stimulation, but do not create peaks in frequency sensitivity.

3.1.3 Time

The behavior of structural vibration in the time domain also has an impact on the human perception. Key areas of interest are dynamic changes in the waveform and a signal's distribution time, i.e. duration or impulsiveness. As an example, understanding the human response to vibration duration can help to understand the difference in sensation caused by a car traveling over a small pothole versus the sensation of a large fan shaking the floor of a building.

T. Miwa proposed an integration time similar to that studied in the auditory system published in an article in *Industrial Health* in 1968 [28]. The author observed that sensation level increased with vibration duration up to 2 seconds for excitation between 2–60 Hz and up to 0.8 seconds between 60–200 Hz. Since that time, studies in whole-body vibration have focused on understanding the relative disturbance of vibrations of different duration and distribution in time. Michael Griffin and Eleri Whitman have proposed a “root mean quad” (r.m.q.) measure to be used in quantifying the disturbance or annoyance of complex vibration [17]. Similar to the “root mean square” value used in many fields, the r.m.q. value shown in Equation 3.3 is a method of averaging over some time duration T . The fourth-order relationship causes impulsive signals (signals with a high crest factor) to be weighted more heavily according to subjective experimentation:

$$\text{r.m.q.} = \left(\frac{1}{T} \int_0^T a^4(t) dt \right)^{1/4}. \quad (3.3)$$

While Griffin and Whitman have shown that the r.m.q. method is a better predictor of subjective disturbance and applies to a signal of any duration, it is not as useful as a time constant for the assessment of arbitrary signals in time. When evaluating musical signals, the researcher would like to be able to compare the human response to different passages. The most useful method of accomplishing this would be to plot an estimate of sensation level versus time, similar to the plot of an A-weighted sound pressure level versus time. In the latter situation, a standard integration time of 125 ms (the “Fast” setting on a sound level meter) has been accepted. No

such integration time has yet been accepted for the assessment of vibration. As a result, this study will present signals in the time domain at instantaneous, absolute amplitude with no integration time.

3.1.4 Other Factors

A number of factors exist that will affect the human perception of vibration independent of the physical characteristics of the signal itself. Surprisingly, footwear has not been found to be one of these factors, even in standing conditions [27]. Many factors that should be kept in mind when considering human response to vibration typical of that experienced in buildings include: the presence of visual or auditory stimuli, posture (knee or back position), the relationship of vibration between seat and footrest, the presence of a backrest in the seated position and seat type (hard or soft) in addition to those listed in Appendix B.

4. Structural Vibration

4.1 Theoretical Mechanics of Motion

The most direct method of describing oscillatory motion responsible for whole-body is to present the wave equation governing displacement for bending waves as shown in Equation 4.1 derived in Fahy and Gardonio's book *Sound and Structural Vibration* for a one-dimensional bar [12] where η represents displacement:

$$EI \frac{\partial^4 \eta}{\partial x^4} = -m \frac{\partial^2 \eta}{\partial t^2}. \quad (4.1)$$

Inserting the complex exponential expression for displacement as a function of time and position as shown in Equation 4.2 results in the relationship between physical properties of the material—Young's Modulus E , second moment area of the cross section I of the neutral axis, and mass per unit length m —and the traveling wave's wavenumber k and frequency ω as shown in Equation 4.3:

$$\eta(x, t) = \tilde{\eta} e^{j(\omega t - kx)}. \quad (4.2)$$

$$EI k^4 = \omega^2 m. \quad (4.3)$$

The fourth-order spatial derivative of Equation 4.1 and resulting relationship shown in Equation 4.3 indicates that bending waves in solids are *dispersive*. In other words, the phase speed of the traveling wave is dependent on frequency, as shown in Equation 4.4. High frequency oscillations will travel through a solid more quickly than low frequency oscillations. The dispersive nature of bending waves sets them apart from other types of waves that travel through solids and those observed in air.

$$c_{\text{bending}} = \omega/k_{\text{bending}} = \sqrt{\omega} \left(\frac{EI}{m} \right)^{1/4}. \quad (4.4)$$

While the wave equation provides useful information about the factors in a structure influencing vibration transmission and the manner in which bending waves travel, the situation becomes much more complex as complex structures including

finite, inhomogeneous materials and geometries come under consideration. The traditional approach to dealing with a complex system is to form a discrete model of the system composed of a network of individual masses, each with an associated set of equations of motion determined by its physical properties and modeled connection to surrounding elements. This method is referred to as the “finite element” approach.

The method, as presented in Ewins’ *Modal Testing: Theory and Practice* [11], as well as Fahy and Gardonio [12], describes the motion of a forced system with hysteric or structural damping¹ in multiple degrees of freedom with the expression shown in Equation 4.5:

$$M\ddot{x} + Kx + jHx = fe^{j\omega t}. \quad (4.5)$$

In this equation, M , K and H represent $N \times N$ mass, stiffness and hysteric/structural damping loss factor matrices, respectively, where N is the number of degrees of freedom in the system. The symbols \ddot{x} , x and f denote $N \times 1$ time varying vectors of acceleration, displacement, and forces. In the case of bending waves, $x = \eta$. N is equal to the number of degrees of freedom assumed for each finite element in the system multiplied by the number of elements in the system. Each degree of freedom represents a direction in which an element is allowed to move or deform. In order to model all types of a wave motion in a solid, six degrees of freedom must be included for each element: x-, y-, and z-axis displacement as well as x-, y-, and z-axis rotation. However, models are often simplified to isolate motion of interest and reduce computational load.

Equation 4.5 results in a set of N equations of forced oscillator motion as shown in Equation 4.6 which describe the displacement of one element in one degree of freedom as a function of force, time, frequency and physical parameters.

$$(K + jH - \omega^2 M)x e^{j\omega t} = fe^{j\omega t}.$$

¹A forced system with hysteric damping is considered here solely for its applicability to the current study in which harmonic forces drive a system that exhibits a damping rate that varies inversely with frequency [11].

or

$$x = (K + jH - \omega^2 M)^{-1} f = \alpha(\omega) f. \quad (4.6)$$

The individual equations of motion and resulting finite element model allow for highly feasible computational models of real systems. These models can predict the response at any point in a mechanical system (or the entire system at once) to single or multiple forces. In regards to music produced stage vibrations, finite element analysis could be used to predict vibration of interest at one listener location resulting from the force created by a musical instrument at another. Because there are many types of instruments and associated complex forcing mechanisms, it would be beneficial to remove the dependence on force from Equation 4.6 in order to quantify the stage's response independent of driving force. The resulting function is called *receptance*.

4.2 Receptance, Mobility, and Accelerance

In one form, receptance can be written by rearranging Equation 4.6 as shown in Equation 4.7:

$$\alpha(\omega) = (K + jH - \omega^2 M)^{-1}. \quad (4.7)$$

However, an expression that is more applicable to measurement and efficient computation can be found by relating receptance to eigenvectors and eigenvalues, otherwise known as mode shapes and resonant frequencies. The first step in finding this equation is to identify the natural resonant frequencies of the system. These eigenvalues can be found in the non-trivial, unforced, undamped solution to Equation 4.5 as shown in Equations 4.8 and 4.9:

$$(K - \omega^2 M) x e^{j\omega t} = 0. \quad (4.8)$$

$$\det|K - \omega^2 M| = 0. \quad (4.9)$$

Substituting the diagonal matrix of eigenvalues back into Equation 4.8 yields an $N \times N$ matrix containing the corresponding eigenvector mode shapes. These two

Table 4.1: Definitions of frequency response functions used in structural modal analysis.

Receptance	$\alpha(\omega) = x/f$
Mobility	$Y(\omega) = \dot{x}/f = j\omega\alpha(\omega)$
Accelerance	$A(\omega) = \ddot{x}/f = -\omega^2\alpha(\omega)$

matrices describe the all of the resonant frequencies and associated physical displacements of the unforced, undamped discrete system. Ewins shows that that a similar set of eigenvalues $[\lambda]$ can be found by solving the unforced, damped Equation 4.5. In the case of hysteric damping, the eigenvalues λ are related to the natural resonant frequencies ω_r by the damping loss factor η_r as shown in Equation 4.10:

$$\lambda_r^2 = \omega_r^2(1 + j\eta_r). \quad (4.10)$$

The damped eigenvalues and eigenvectors can be used to rewrite Equation 4.7 as shown in Equation 4.11:

$$\alpha_{jk}(\omega) = \sum_{r=1}^N \frac{r\psi_j r\psi_k}{\omega_r^2 - \omega^2 + j\eta_r\omega_r^2}. \quad (4.11)$$

Equation 4.11 is quite useful in that it is dependent on resonant frequencies, mode shapes and damping loss factors which can be readily obtained from measurements of existing structures. The measurement of modal frequencies and shapes can then be used to describe the response of a real system to an arbitrary force as shown in Equation 4.12 with mass-normalized eigenvectors:

$$x = \sum_{r=1}^N \frac{\phi_r^T f \phi_r}{\omega_r^2 - \omega^2 + j\eta_r\omega_r^2}. \quad (4.12)$$

Once receptance has been obtained, mobility and accelerance can be evaluated through the simple relationships shown in Table 4.1.

4.3 Measurements

The process of measuring modal resonances, mode shapes, and damping loss factors is called modal analysis. Many advanced measurement techniques have been

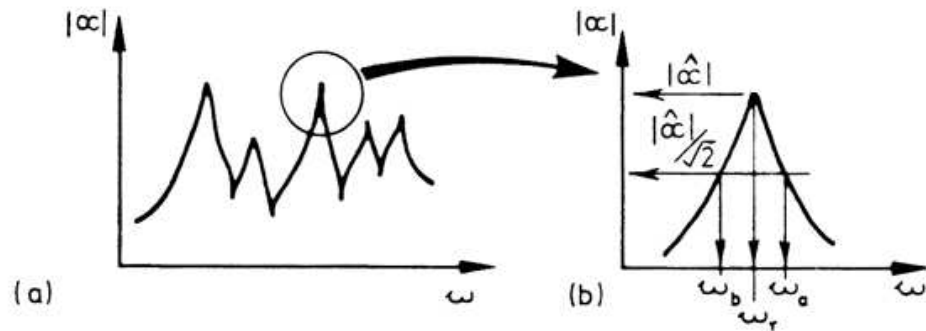


Figure 4.1: a) Typical receptance frequency response function showing modal resonances. b) Detail of single resonant peak. Damping ratio is dependent upon the height and bandwidth of the peak. Taken from *Modal Testing: Theory and Practice*

developed and are discussed in Ewins' book [11]. In all methods, the objective is to obtain the system's response to a known input force in the frequency domain at a resolution sufficient enough to properly identify frequencies and damping factors as shown in Figure 4.1. Mode shapes are obtained by making many measurements across a structure in a grid and using the differences in response normalized by input force. Figure 4.2 shows a simple example of a grid and resulting (exaggerated) displacements used to calculate a mode shape.

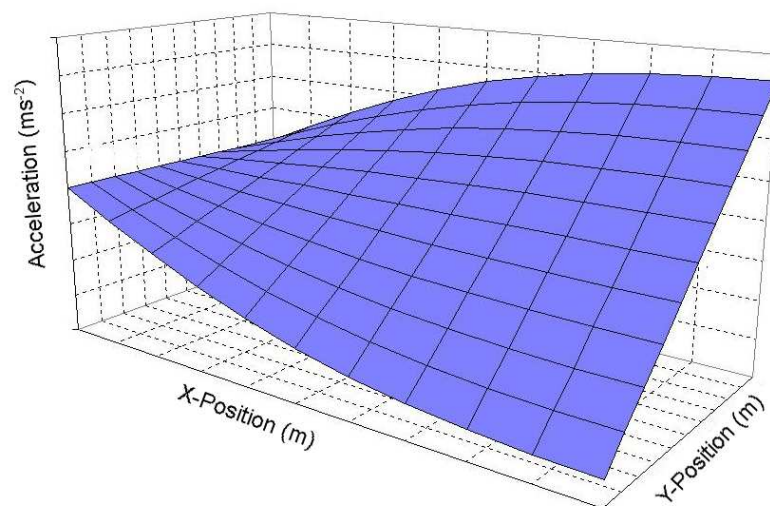


Figure 4.2: Example mode shape. Acceleration is exaggerated for easy identification of nodes and antinodes.

5. Experimental Design

Two primary objectives are considered in the experiment presented in this paper: (1) to measure and compare the physical vibration created on common orchestral stage constructions during a musical performance and (2) to evaluate the characteristics of stage vibration that control perceptual differences. This section discusses the following steps taken to accomplish these objectives:

- Record vibration created on a stage by a contrabass performing a musical passage in a coupled and uncoupled condition
- Measure the mechanical response of five stage constructions using modal analysis techniques
- Use the mechanical impulse responses and uncoupled vibration to create musical vibration signals that are experienced at each stage measurement location by convolution
- Present the audio and tactile signals to listeners using an audio-tactile display
- Ask subjects to rate perceived differences between signals in an A/B comparison
- Use multidimensional scaling to explore the physical characteristics underlying perceptual differences

Experimental procedures are discussed for data collection, development of the audio-tactile display and psychoacoustic test methods.

5.1 Data Collection

Prior to beginning the in depth study of differences in stage vibration, the author is first interested in confirming that a musical instrument performed on orchestral stages generates enough force to excite perceivable vibration at typical listening distances. A simple pilot study was conducted on the stage at the Experimental

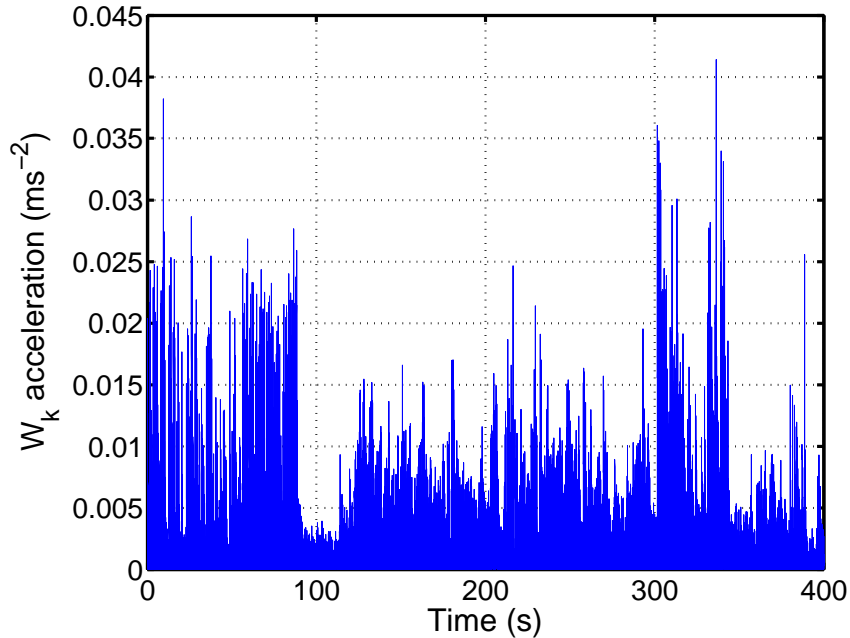


Figure 5.1: Peak frequency weighted acceleration measured at 2 m on the Slab-A concrete slab stage construction during a musical contra bass performance. Absolute threshold of perception is approximately $0.01 \text{ ms}^{-2} W_k$.

Media Performing Arts Center (EMPAC) Concert Hall in Troy, NY. Michael Bullock performed several musical passages on the contrabass supported by the stage in a traditional manner while vibration waveforms are recorded at a distance of 2 meters. Figure 5.1 shows the instantaneous, absolute peak vibration measured during 400 seconds of the musical performance. Stage vibration is recorded with a PCB Piezotronics 333B50 accelerometer (see Appendix E for equipment specifications).

Approximately 2.4% or about 9.5 seconds of the measured signal exceeded the threshold of probable sensation at $0.01 \text{ ms}^{-2} W_k$ peak. Above this level, perceptible vibration reached amplitudes of up to $0.04 \text{ ms}^{-2} W_k$ peak. Peak acceleration levels are used in order to maximum compatibility with other results and avoid inconsistencies that occur when averaging methods such as r.m.s. or r.m.q. are used, as suggested by Griffin [18]. Sensation levels associated with these magnitudes would range from “probably perceptible” to greater than “very strong perception” as shown in Table 3.1. The implication of the measured distribution and magnitudes is that

vibration is important for perception only during the strongest portions of performance, in this case the attack portion of notes. However, the vibration generated results in highly perceptible levels of sensation. The measurements presented in this section also serve as a guideline for level calibration of the audio-tactile display.

5.1.1 Musical Source Material

Previous studies in audio-tactile music perception have been conducted using single note source material recorded during a performance in an effort to minimize differences between stimuli in musical content and performance [10], [23]. In this study, there exists a desire to present musical source material in its most natural form, such as a short musical passage with no restrictions on performance. A technique inspired by the anechoic musical recordings used in computer auralizations is used to eliminate inter-stimulus differences.

The first task in this process is to obtain vibration created by the instrument that is not affected by the supporting surface it is performed on. In practice, this turns out to require less effort than obtaining anechoic recordings. The contrabass is supported by a small platform, roughly the size of the peg, that is isolated from the floor by a spring/damper system as shown in Figure 5.2. Vibration generated by the instrument is then measured next to the peg on the platform with the PCB Piezotronics 333B50 accelerometer.

The resonant frequency of the combined mass/spring/damper system is measured at approximately 7 Hz. The result of isolation and damping is that acceleration generated by the instrument situated on the platform will be minimally impacted by stage response above 35 Hz (approximately 5 times the resonant frequency as suggested by Ewins [11]). The method used in this study may also be used in the future to evaluate the relative contributions of structure-borne versus airborne excitation of structural vibration [30].

A Head Acoustics HMS V.II binaural dummy head measurement system is used to record the audio portion of the musical performance at 2 meters in front of the contrabass player facing the musician on the EMPAC stage. Other audio measurement conditions more familiar to orchestral seating were considered, but

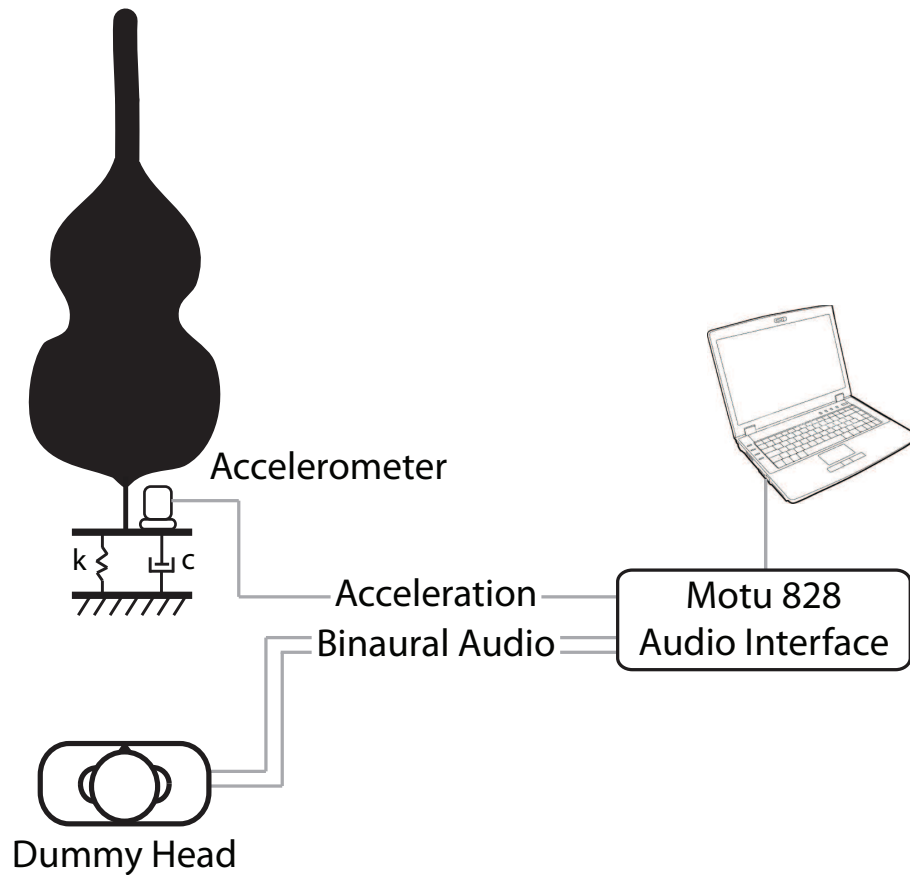


Figure 5.2: Diagram of musical source material recording system. Binaural audio is recorded with a Head Acoustics HMS V.II dummy head, the contrabass is isolated from influence of stage vibration by a spring/damper system and recorded with a PCB 333B50 accelerometer.

this location has been selected due to ease and naturalness of the listening task presented with the audio-tactile display.

5.1.2 Stage Structural Response

The structural responses of five stage constructions are measured: two stages constructed with wood beams and joists and a thin wooden subfloor below a finish floor; two stages constructed with a wood finish mounted on sleepers supported by a thick concrete slab; and one hydraulic pit riser. Architectural details of each stage construction can be found in Appendix C. Structural responses are measured with the intention of quantifying the following properties:

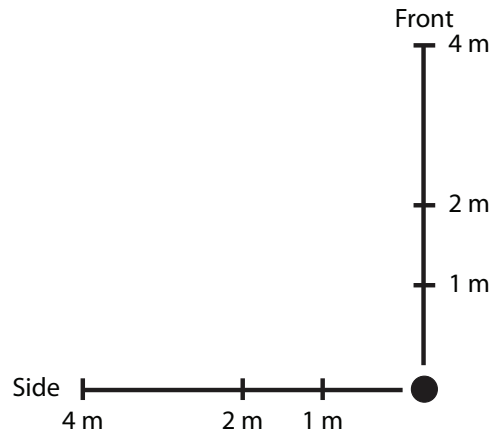


Figure 5.3: Structural response measurement locations. Dashes mark source positions, black circle marks receiver position.

- The physical magnitude of vibration generated by a known force in the frequency range important to the human perception of vibration (0 to 100 Hz).
- The change in vibration with distance and direction on each stage.
- The change in vibration response controlled by stage characteristics such as finish material or structural design.

A measurement technique designed for use in modal analysis is employed at six locations on each stage construction as shown in Figure 5.3². Structural response is measured by accelerance, as defined in Section 4.2, using an impulsive source. An instrumented sledge hammer is used to create and measure a broadband input force while a Polytec PDV-100 laser doppler vibrometer is used to measure the vibration response (acceleration calculated by integrating the measured velocity) as shown in Figure 5.4.

The transfer function between force input and acceleration output in the frequency domain as shown in Equation 5.1 represents the frequency dependent accelerance function where F represents force and a represents acceleration:

$$A(f) = \frac{FFT\{F(t)\}}{FFT\{a(t)\}}. \quad (5.1)$$

²One stage construction is a narrow pit riser along which only one direction of measurements could be made, resulting in three data points. One measurement location at 4 meters in the forward direction on the EMPAC stage is missing due to technical difficulties.



Figure 5.4: Structural impulse response measurement equipment. Instrumented sledhammer used to measure force input, laser doppler vibrometer used to measure force output (isolated from stage with bungee cord). Not Shown: 150 lbs of sand placed on chair used to mass load receiver position, source position mass loaded by experimenter operating hammer.

As discussed in Section 2.3 previous studies have shown an interest in time delays between audio and tactile signals [10],[23]. The structural impulse responses measured in this study allow a comparison to be made between the conditions used in these previous studies and time delays occurring in real-world situations. The cross-correlation function between the force input and acceleration output measured for the impulse response is used to identify the vibration propagation time between source and receiver. The arrival time is chosen to be the time at which the maximum of the absolute value of the cross-correlation function occurs. The discrete cross correlation function is shown in Equation 5.2.

$$(f \star g)[n] = \sum_{m=-\infty}^{\infty} f^*[m] g[n + m]. \quad (5.2)$$

In this study, force input is estimated by measuring the acceleration generated by the hammer with a PCB Piezotronics 308B03 accelerometer and assuming a constant mass of the sledge hammer head. In an ideal situation, force would be measured directly with a force transducer. However, the resulting errors would be in calculating the overall scale of the force input to a reference value such as 1 Newton. Relative changes in energy transfer as a function of frequency would remain accurate and can be compared between one another because the same mass is used in each measurement. As a result, accelerance values presented in this paper are evaluated only in a relative manner and any comparison of the values with other test data should be done so with caution. See Appendix E for equipment specifications.

Vibration signals matching those experienced at each of the 26 measurement positions are created by convolving the uncoupled vibration signal with the structural impulse responses using the method shown in Equation 5.3.

$$(f * g)[n] = \sum_{m=-\infty}^{\infty} f[m] \cdot g[n - m] \quad (5.3)$$

The full list of construction types and measurement locations are provided in Appendix C.

5.2 Audio-Tactile Display

Audio and tactile signals must be presented to listeners in a manner that is both plausible and adjustable to match experimental parameters. Historically, two methods of presentation have been accepted: (1) placing listeners in real world situations and evaluating results based on net differences in physical parameters and (2) using a plausible virtual display. The benefits and drawbacks of each method have been widely discussed and are presented in the following papers: [4], [13], [7], [24]. A summary of the tradeoffs is that placing listeners in actual listening conditions provides the most accurate representation at the expense of the ability to isolate and control separate variables, while using a virtual display sacrifices fidelity and the completeness of a real environment. In this study, the need exists to adjust vibration independent of visual and audio cues, a feat impossible using real world conditions. This section presents the design and details of the audio-tactile presentation developed for this experiment.

5.2.1 Motion Platform

Tactile signals are presented to the listener via a Buttkicker electrodynamic shaker mounted to the bottom center of a motion platform as shown in Figure 5.5. The shaker is powered by a 1000-watt amplifier. A hard, wooden chair is rigidly attached to the top of the platform.

A calibration process is conducted to minimize the impact of the structural response inherent to the platform itself on signals presented to the listener. Heavy wood construction and extensive bracing are used to make the platform as stiff as possible and raise the natural resonances to a frequency range above that important for human perception. Once the platform is constructed, the frequency response is measured at several locations on the top of the platform and bottom of seat with a 180-lb subject sitting in a relaxed position on the platform. As expected, frequency response varied with location due to the complex structure. The bottom center of the seat is selected for the calibration and measurement location due to its maximum contribution to the vibration transmitted to the body.



Figure 5.5: Motion platform used in multimodal presentation of audio-tactile stimuli. Sennheiser HD280 headphones are used for audio presentation.

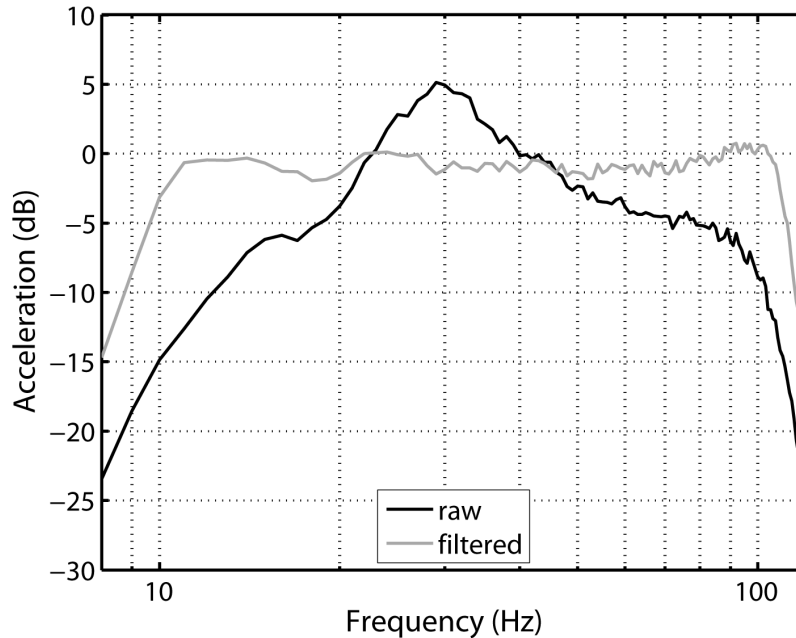


Figure 5.6: Frequency response measured at the bottom of hard wooden seat mounted to the motion platform before and after calibration. Measurements are made with a 180 lb human subject seated on the platform.

Figure 5.6 shows the frequency response of the bottom of the platform seat before and after frequency response calibration with a 180-lb human subject seated on the platform. Equalization is accomplished by a minimum-phase, inverse FFT filter and occurs offline before presentation. Band limiting of the platform is set by a high-pass filter at 30 Hz and a low-pass filter at 100 Hz due to the capabilities of the shaker/platform system and the lowest frequency generated by the contrabass - approximately 40 Hz. The time delay between an audio signal at the subject's ear and a tactile signal at the bottom of the seat is measured by taking the transfer function between the output of a dummy head wearing the headphones and an accelerometer attached to the seat bottom. The 3-ms time delay observed (vibration lagging) is corrected for by adding a 3-ms delay to audio signals during presentation.

Amplitude calibration is accomplished by matching the r.m.s. acceleration of a signal generated by convolution with a signal recorded on the stage directly as presented in Section 5.1. A 30 second sample generated by convolving the uncoupled vibration with the 2 meter forward direction EMPAC stage mechanical impulse

response is compared to a 30 second measurement made in the same location on the same stage with the contrabass supported by the stage. Because the vibration generated by the bass could only be recorded with an accelerometer, actual force input levels to the stage are currently unknown. The level and frequency calibration process used ensures inter-stimulus differences in level, frequency, and time are reproduced accurately. The correlation to actual levels that would be measured on each stage can only be represented as approximately and within the range of plausibility. As a result, correlation between stimulus characteristics and subjective response are analyzed using signals recorded *on the platform* during experimentation.

5.2.2 Binaural Audio

In this study, audio is presented as a reference by which subjects can ground their perception of vibration. The audio environment maintains fixed across all tactile signal comparisons. Subjects are not asked to analyze the audio environment. As a result, the primary concern in the audio portion of this test is plausibility. That is, the subjects should feel as if the audio environment accurately represents the one they might experience if they were sitting in front of the bassist on the stage.

Binaural recording and playback techniques are employed for the presentation of audio in the audio-tactile display. The theory and application of binaural techniques are presented in depth in Jens Blauert's *Spatial Hearing* and summarized in this section [6]. A binaural microphone system consisting of a dummy head and two microphones located at the ear canal entrances is used to capture the interaural time and level differences that the human auditory system uses for localization in the horizontal plane. When played back via headphones, these signals accurately represent the spatial qualities of a sound field, resulting in a heightened sense of perceived reality. In a more complex system, head-related transfer functions (HRTFs) representing the frequency response function of the actual listener's torso, head and pinnae of sources from different directions would be included via a filtering process. This step, which helps moved the perceived location of sources outside the head, is not necessary for this experiment, but may be included in future research.

The headphone amplification system is calibrated such that signals are presented to the listener at the exact levels recorded, by method described in the HEAD Acoustics application note [19]. Closed-ear Sennheiser HD280 headphones used for audio presentation are selected for quality and to isolate noise generated by the platform. Amplification levels are limited such that A-weighted sound pressure levels do not exceed 80 dBA.

5.3 Subjective Testing

This study marks one of the first experiments in the overall perception of musical vibration in the presence of sound. One of the primary objectives is to explore the dimensions of perception to see what characteristics of the signals govern subjective responses. A psychometric procedure called multidimensional scaling (MDS) is selected to explore the subjective responses. This procedure is a popular choice for the exploration of subjective qualities and has been employed in past studies into the perceptual dimensions of timbre [16] and preference for concert hall acoustics [35].

5.3.1 Multidimensional Scaling

5.3.1.1 Definition

Multidimensional scaling (MDS) is a method for exploring the underlying factors or “structure” of a data set. It is an exploratory data analysis technique in which an iterative process is used to find a mathematical transformation that maps a set of distances between objects or stimuli into an m -dimensional space in which Euclidean distances approximate the input distances. In a typical introductory example, MDS is used to recreate a two-dimensional map given an input table of distances between cities [22].

The benefits of MDS are that test stimuli can be presented in their naturally occurring form and the influence of experimental design on subjective responses is minimized. Test subjects are simply presented with two stimuli and asked to provide a single value “difference” between the two. The experimenter is not required to

Table 5.1: Sample difference matrix used in Multidimensional Scaling. Each cell represents the perceptual difference between the stimulus associated with row i and column j .

Stim. #	1	2	3	4	5	6	7	8	9	10	11	12	13	14
1	-	3	2	1	3	1	2	5	1	2	4	2	2	6
2	3	-	4	5	6	4	5	6	4	5	2	2	3	5
3	2	4	-	4	3	1	2	3	3	1	5	4	6	7
4	1	5	4	-	6	5	5	6	3	4	4	1	3	3
5	3	6	3	6	-	2	2	3	6	5	6	6	6	6
6	1	4	1	5	2	-	1	3	4	3	6	5	6	7
7	2	5	2	5	2	1	-	3	1	1	5	4	3	7
8	5	6	3	6	3	3	3	-	3	3	7	6	6	7
9	1	4	3	3	6	4	1	3	-	1	4	3	4	6
10	2	5	1	4	5	3	1	3	1	-	3	4	5	6
11	4	2	5	4	6	6	5	7	4	3	-	1	2	2
12	2	2	4	1	6	5	4	6	3	4	1	-	3	6
13	2	3	6	3	6	6	3	6	4	5	2	3	-	5
14	6	5	7	3	6	7	7	7	6	6	2	6	5	-

pre-select a set of attributes to be studied, as in a related method called factor analysis [21].

The input to an MDS model is a difference matrix. Each row and column of the matrix represents an object or stimulus. The matrix is populated with subjective “differences” or “proximities”. A sample matrix taken from this study is shown in Table 5.1.

From the set of differences, MDS creates an m -dimensional space in which the objects labeling the difference matrix are given coordinates. The dimensionality m is defined by the user. The Euclidean distance between these coordinates, shown in Equation 5.4, are given by a transformation to equal the input data plus an error value [8]. x_{ia} and x_{ja} represent the stimulus coordinate in dimension a for proximity ij and d_{ij} represents the calculated distance:

$$d_{ij}(\mathbf{X}) = \left[\sum_{a=1}^m (x_{ia} - x_{ja})^2 \right]^{1/2}. \quad (5.4)$$

The purpose of MDS is to find a transformation that matches these distances as shown by f in Equation 5.5 where p_{ij} represents the input proximities and d_{ij}

the distance defined by the transformation. The form that f takes defines the type of MDS model. The transformation f is selected by the user based on guidelines provided by empirical data [22], [31], [8]:

$$f : p_{ij} \rightarrow d_{ij}(\mathbf{X}). \quad (5.5)$$

Two popular MDS models are *interval* and *ordinal* MDS. In interval MDS, the transformation is defined by a linear function as shown in Equation 5.6 [8] where a and b are free to be adjusted by the model. Interval MDS falls under the broader category of *metric* MDS transformations. Metric MDS models are defined by a transformation maintaining a strict mathematical relationship:

$$p_{ij} \rightarrow a + b \cdot p_{ij} = d_{ij}(\mathbf{X}). \quad (5.6)$$

Ordinal MDS is defined by a simple monotonic function that preserves the order of distances. That is, all greater-than and less-than relationships are maintained. The ordinal transformation is defined by the following relationship:

$$\text{if } p_{ij} < p_{kl}, \text{ then } d_{ij}(\mathbf{X}) < d_{kl}(\mathbf{X}). \quad (5.7)$$

If two input proximities are equal ($p_{ij} = p_{kl}$), called a “tie”, a decision must be made whether to maintain the equality in the MDS configuration, or to ignore the equality allow relationship between the two equal proximities to be defined by other proximities. The latter in which “ties are broken” is identified as the *primary approach* and the former the *secondary approach*. The primary approach is often the most appropriate when proximities are based on a perceptual scale because the equality occurs due to the use of a discrete rating scale where the perceptual scale is continuous [31].

Of course the transformation model selected will not result in a set of Euclidian distances that are equal to proximities for all pairs of stimuli. Thus, the notion of error is introduced. The error of representation is defined by Equation 5.8:

$$e_{ij}^2 = [f(p_{ij}) - d_{ij}(\mathbf{X})]^2. \quad (5.8)$$

The first and most commonly used goodness-of-fit measure is defined by summing the squared error function over all proximity/distance $f(p_{ij})/d_{ij}$ pairs and normalizing by the transformed distance d_{ij} . The resulting value is Kruskal's *Stress-1* as defined in Equation 5.9 [8]. Stress-1 is used in the iteration process to select the transformation used in defining the final stimulus space configuration.

$$\text{Stress-1} = \sigma_1 = \sqrt{\frac{\sum [f(p_{ij}) - d_{ij}(\mathbf{X})]^2}{\sum d_{ij}^2(\mathbf{X})}}. \quad (5.9)$$

The use of an ordinal transformation allows the scaling procedure to fit a model to the data without the assumption of linearity. Model distances are optimized such that they match the rank order of perceptual distances. In practice, researchers have found that the use of ordinal or metric scaling techniques often has little impact on the resulting model configuration [31]. The metric configuration will have a higher “stress” due to larger residual errors that may occur from fitting a linear model to a non-linear system.

5.3.1.2 Application

A typical course of action in gathering subjective data for use in multidimensional scaling is outlined below:

- Present subjects with stimuli in pairs, making sure each pair of stimuli is tested³.
- Ask subjects to provide a single rating of the *difference* between the two stimuli encompassing their overall perception of the stimuli.
- Create a matrix for each subject in which the difference between two stimuli is located at the row i and column j for the stimuli pair ij .

The set of difference matrices can be analyzed in one of two ways. The first option is to average all the matrices into a single difference matrix to be used in

³The possibility of using multidimensional scaling to evaluate incomplete difference matrices has been evaluated by Spence and Domoney [33]. Their findings indicate data becomes highly inaccurate with less than approximately 40 stimuli (high relative to this study) or even a marginal amount of error in the data (approximately 15%).

a *two-way* MDS configuration [31]. The second option is to use *three-way* MDS to create individual MDS configurations for each matrix as well as a combined group configuration and “subject space”. The group configuration is related to individual configurations in that each individual matrix can be obtained by “stretching” the group space by a scalar value for each dimension/axis. These scalar values can be plotted in vector form to show the relative contribution or importance of each dimension to the individual subjects’ ratings called the subject space. For this reason, the case of three-way MDS in which the third mode (the addition of multiple matrices) represents individual subjects in a subjective test is referred to as an Individual Difference Scaling procedure. An interesting effect of the individual difference scaling procedure is that the group stimulus space can not be rotated, resulting in one less variable to explore in the interpretation of the spaces.

MDS configurations are computed using the SPSS statistical analysis software package version 16.0. SPSS implements the ALSCAL multidimensional scaling algorithm developed by Forrest Young. Both two-way and three-way ordinal configurations are computed with “ties broken.”

Stress-1 is used to evaluate the fit of the model. A typical methodology is to calculate several models of different dimensionalities m and plot their stress values in ascending order of dimensionality. Ideally, the resulting “scree-plot” will have a knee at which the model has obtained the highest level of fit, and any further decrease in stress represents an improvement in the model’s fit of noise in the data. The dimensionality at which the knee occurs should represent the true dimensionality of the data. It is not uncommon for the scree-plot to lack a knee. In this case, Monte Carlo methods are employed to compare the stress obtained with experimental input data to the stress obtained when fitting random noise [8]. At minimum, the experimental data’s stress should be less than that of noise. Beyond these tests, a rule of thumb scale has been proposed and is presented in Table 5.2.

Stress should always be considered with an estimate of noise in the data. It is possible for an MDS to accurately represent the dimensionality of a data set despite a high stress value due to noisy data. Alternatively, a low stress value may simply indicate a high level of fit to erroneous data.

Table 5.2: Rules of thumb for evaluating Kruskal’s Stress-1 goodness-of-fit measure [8].

Fit	Kruskal Stress-1
Poor	0.2
Fair	0.1
Good/Excellent	0.05
Perfect	0

Once a proper MDS configuration is obtained the user is responsible for interpreting the meaning of the axis. One method of interpretation is regression analysis, as suggested by Schiffman, Reynolds and Young [31] and as conducted by Yamaguchi and Schroeder, Gottlob and Siebrasse [35], [32]. Regression can be used to evaluate the correlation between perceptual axis identified by MDS and physical parameters of the stimuli. Linear regression assumes that an independent variable can be used to predict a dependent variable based on a linear relationship, as shown in Equation 5.10. Two-way MDS configurations can be rotated or translated in order to identify the proper correlation.

$$Y = a \cdot X + b \quad (5.10)$$

The method of least squares is used to determine the slope a and intercept b of the line used to model the dependent variable. The model in Equation 5.10 can be expanded to include several variables, called multiple linear regression as shown in Equation 5.11. Technically, the use of ordinal MDS does not guarantee a linear scale of the perceptual values. However, linear regression provides a simple and useful method of identifying correlations despite the complex relationship between the physical and perceived worlds.

$$Y = \beta_0 + \beta_1 X_1 + \beta_2 X_2 + \dots + \beta_n X_n. \quad (5.11)$$

The coefficient of regression R^2 is used to assess the goodness-of-fit of the model. A related value, the Pearson product moment coefficient of correlation p can be used to measure the extent to which the independent and dependent variables are correlated. In this study, a high coefficient of correlation indicates a connection between perceptual dimensions and physical parameters.

Table 5.3: Stimuli used for Subjective Experimentation.

Stimulus #	Stage Construction	Meas. Dist. (m)	Direction
1	Slab-A	1	Front
2	Slab-A	2	Front
3	Slab-A	1	Side
4	Slab-A	2	Side
5	Slab-B	1	Front
6	Slab-B	2	Front
7	Slab-B	1	Side
8	Pit Riser	1	Side
9	Pit Riser	2	Side
10	Joist-B	1	Front
11	Joist-B	2	Front
12	Joist-B	1	Side
13	Joist-B	2	Side
14	Joist-B	4	Side

5.3.2 Subjective Testing

A total of 26 structural impulse responses are measured for five different stage constructions. The 26 impulse responses are used to create 26 tactile signals that would be perceived at each measurement location as described in Section 5.1.1. The number of pairs required to complete a full difference matrix is given by $n(n-2)/2$ where n is the number of stimuli. 26 stimuli would result in 325 pairs. If subjects chose to listen to the entire 2 minute musical sample, using all the stimuli would result in a test that would take 10 hours and 48 minutes. Such a duration is highly undesirable, resulting in the need to eliminate some stimuli from the experiment.

A simple methodology is used to select 14 of the stimuli for use in the perceptual test. After evaluating all of the structural impulse responses, an estimate is made of the r.m.s. acceleration amplitude of the first 30 seconds of the musical sample. Twelve of the stimuli indicated a level at or below the threshold of perception and are thus eliminated. The resulting 14 stimuli are listed in Table 5.3 along with their associated stage constructions and measurement locations. The elimination process is based on estimates of levels that would be generated by the platform and should not be interpreted to mean that perceptible vibration would not occur at the measurement locations eliminated.

The 14 stimuli selected are presented to listeners using the audio-tactile display described in Section 5.2. Listeners use a simple computer interface implemented in Max/MSP software controlled by a hand-held input device to run the experiment. An image of the interface is shown in Figure 5.7. The user is able to switch back and forth between a current pair of stimuli in real-time while listening to the musical passage. The user can also restart the passage at the beginning. The subject is allowed to listen to as much of the 2 minute passage as they like before making a decision as to the difference rating. Once decided, the listener selects a difference rating from 1–7 and moves to the next pair of signals.

Each subject is presented with a total of 91 pairs of stimuli in A/B comparison format. Signals are not tested against themselves. The presentation order of stimuli is randomized and broken up into three segments (two of 30 stimuli and one of 31). The order of stimuli in each segment remains the same, but subjects take the three segments in a randomized order. The subject is asked to complete 5 trial tests to become familiar with the system and differences between stimuli. A copy of the instructions provided to subjects in the Institutional Review Board approved Informed Consent Form can be found in Appendix D.

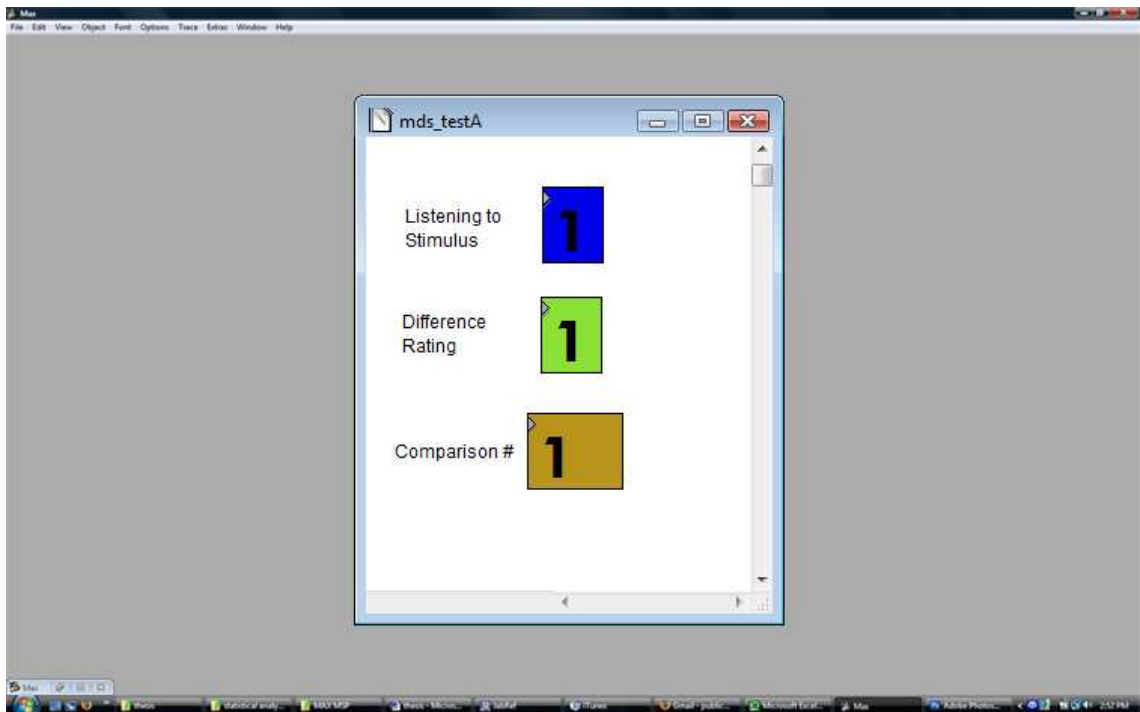


Figure 5.7: Computer interface used by subjects to operate experiment. Number values on the screen are controlled by a handheld video game controller.

6. Results and Analysis

Experimental data and results of analysis are presented in two parts: the first discussing structural response measurements and the second covering subjective testing. Each section will present an example of raw data measured as well as an analysis of the data with regard to the objectives of this experiment.

6.1 Structural Response

An example of an impulse response measured on a stage construction in both the time and frequency domains is shown in Figures 6.1 and 6.2.

The general form of the impulse response shown in Figures 6.1 and 6.2 are typical of all stage impulse response measurements. Each impulse response measured

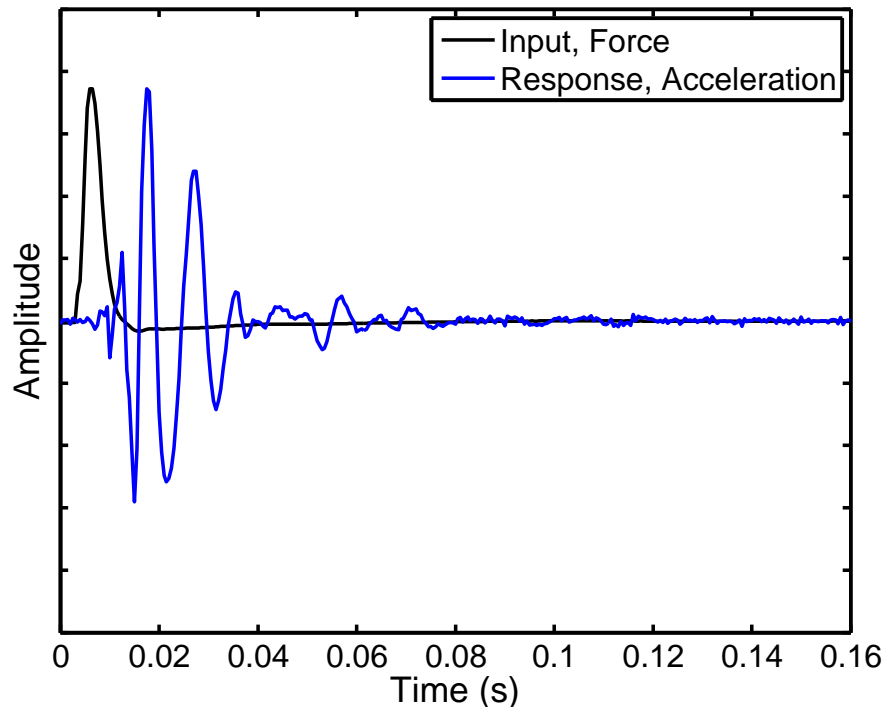


Figure 6.1: Sample structural impulse response in the time domain measured at 2 m on the Slab-B construction in the sideways direction. Amplitudes are scaled so that their absolute maxima are equal.

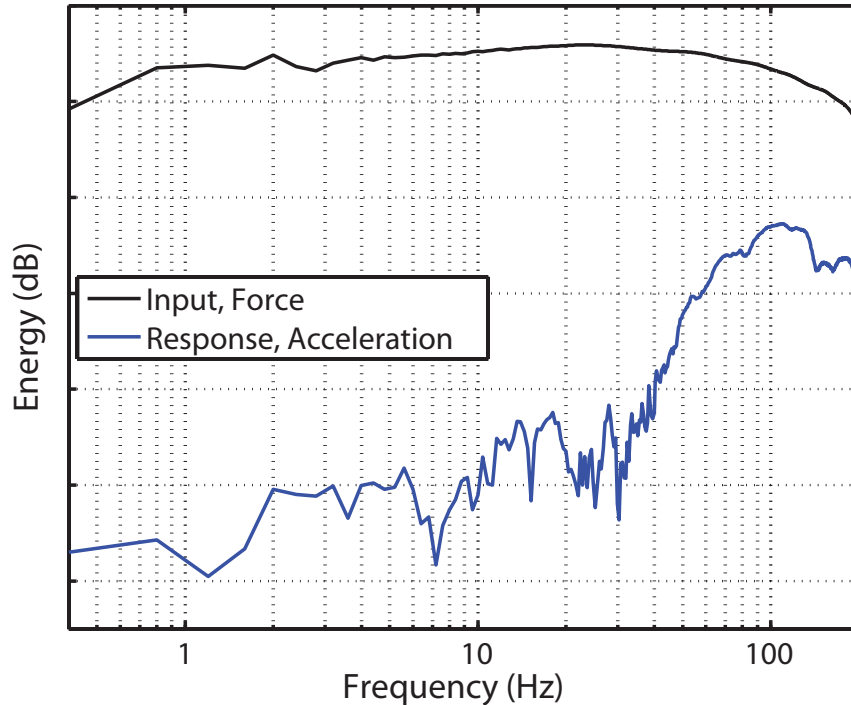


Figure 6.2: Sample structural impulse response in the frequency domain measured at 2 m on the Slab-B construction in the sideways direction. Magnitude spectra represent the square amplitudes of force and acceleration.

shares the same frequency range. The frequency range of the force input determines the range of validity for output data and is shown to be approximately 10 Hz to 100 Hz. Input force rolls off above 100 Hz due to the hardness characteristics of the hammer and wood puck upon which it is struck. Data below 10 Hz becomes unusable due to a combination of decreasing excitation of the structure and the noise floor of the measurement equipment. The lowest frequency generated by the contrabass is measured at 41 Hz. The upper frequency limit extends well beyond 100 Hz, but is not expected to be important due to human frequency sensitivity to whole-body vibration.

Each subsection below presents results of all structural impulse responses measured from the perspective of vibration magnitude, frequency content and temporal characteristics.

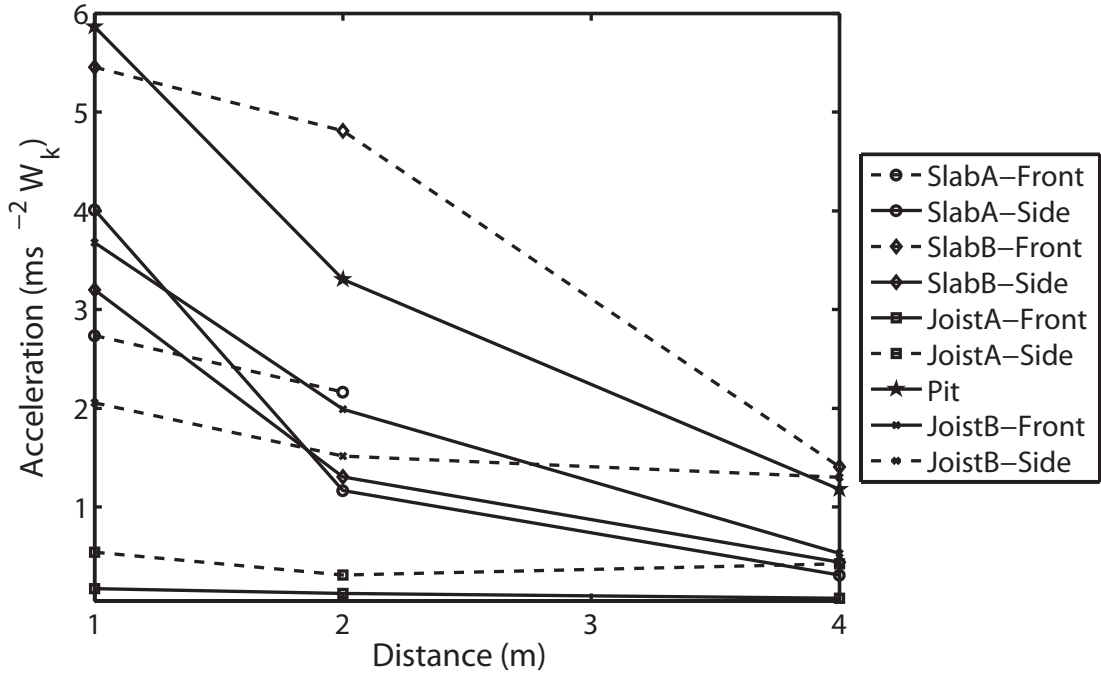


Figure 6.3: Stage vibration response as a function of distance.

6.1.1 Magnitude

Vibration response magnitude is presented in two forms: raw acceleration and frequency weighted acceleration. Frequency weighted acceleration is presented and analyzed as representative of the sensation level experience by subjects. The frequency weighting curve used is W_k as defined in ISO 2631 and discussed in Section 3.1.2. Table F.1 in Appendix F presents the acceleration and W_k acceleration measured at each position. Figure 6.3 presents frequency weighted acceleration as a function distance. Each value represents the total energy between 10 and 100 Hz generated on a stage by a 1 Newton impulse force.

A review of the data presented in Figure 6.3 indicates that vibration magnitude does not decrease linearly with distance. Figure 6.4 shows a plot of \log_{10} of the acceleration values versus distance. The data in Figure 6.4 is presented as a scatter plot with linear regression lines to show the trend of decreasing vibration with distance.

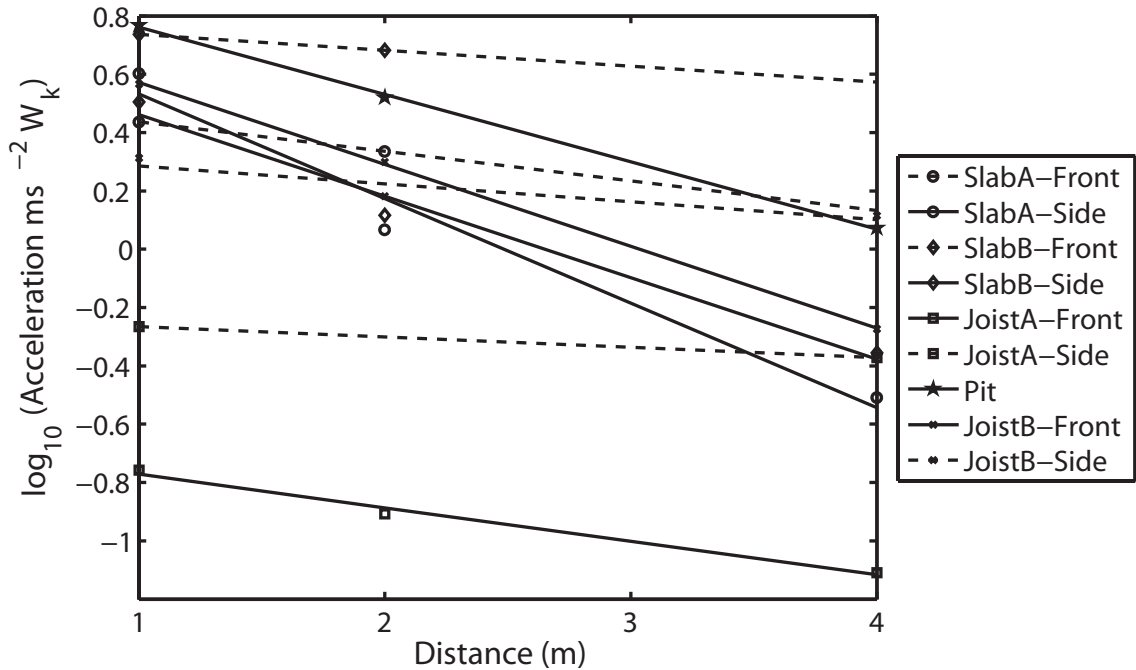


Figure 6.4: \log_{10} of stage vibration response as a function of distance. Individual measurements shown with linear regression lines.

Two data points are identified as outliers and eliminated from Figure 6.4. One of the outlying data points is measured with the force input directly above a structural beam and the other with the force input within a decimeter of the edge of a floor (close to the point at which the floor supports a wall). Acceleration response at both of these locations is found to be significantly lower than the attenuation-with-distance trend observed for all other measurement sets.

With outlying data points eliminated, a linear regression line can be fit to all data sets with an absolute coefficient of regression of greater than 0.93. An interesting phenomenon observed is that there appears to be two sets of slopes, with each stage having one slope from each category. The data are split into two groups and a two-tailed, two sample t-test is used to test the alternative hypothesis that two groups have different means. The null hypothesis that both sets of data have the same mean value is rejected at the 99% confidence level with a significance of $p = 0.005$ or 0.0068 (depending on whether the two sets of data are assumed to have equal or different variance), indicating two statistically significant attenuation

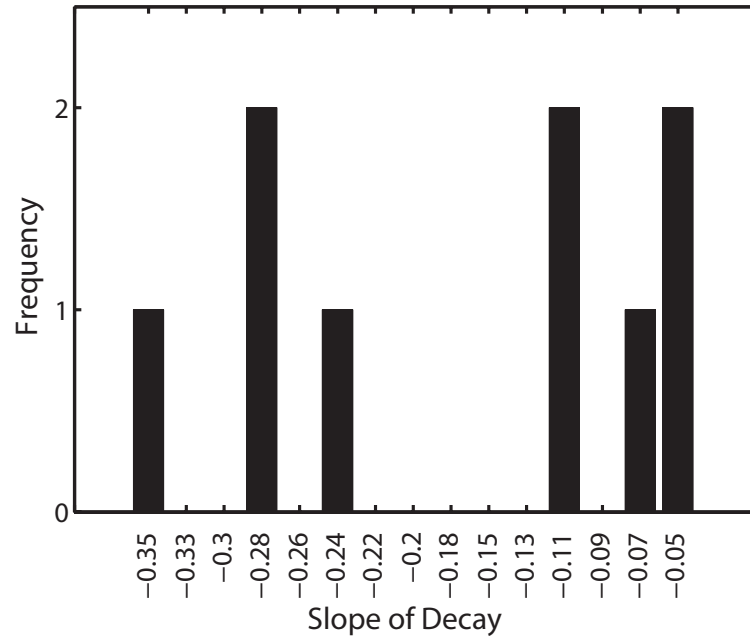


Figure 6.5: Histogram of slopes observed in linear regression of logarithmic acceleration data plotted against distance.

slopes are observed. A histogram of attenuation slopes observed is plotted in Figure 6.5.

6.1.2 Frequency

Each point for which vibration magnitude is measured has an associated frequency response representing acceleration in response to force input. The frequency response plot is used in modal analysis to identify the frequency, magnitude and bandwidth of natural resonances observed at a specific point in a structure. Perceptually, the frequency response contains information about the “tonal” makeup of the stage vibration at a specific point. Two examples of structural frequency responses are shown in Figure 6.6. The “Joisted Stage” response shown in Figure 6.6 is measured at 2 meters along the joists on Joist-A construction. The “Slab Stage” response is measured at 2 meters across the sleepers on the concrete Slab-A.

Figure 6.6 presents the two types of responses observed. The joisted stage shows a modal or “peaky” type response typical of all the joisted wood stages and orchestra pit riser. The slab stage shows a damped or “smooth” frequency response

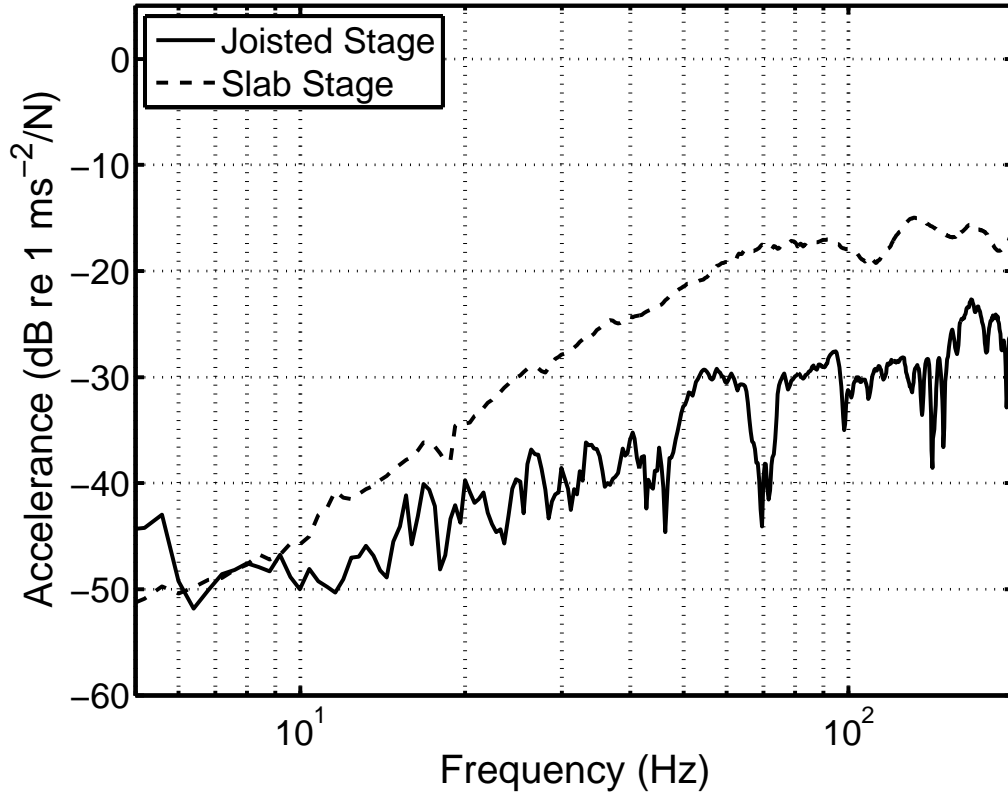


Figure 6.6: Modal and non-modal acceleration frequency response functions typical of joisted and concrete slab stage constructions, respectively.

typical of all the concrete slab constructions. All frequency response functions measured are included in Appendix G.

6.1.3 Time

Structural impulse responses are also evaluated in the time domain. The impulse response in Figure 6.1 shows that as time progresses after the impact, the induced bending wave travels through the receiver point. The structure begins to move initially with small displacement and high frequency oscillations. It then reaches a maximum acceleration controlled by a rise time followed by period of “ringing” at a lower frequency. The result is an impulse response in which energy at different frequencies is spread out in time. Reasons for this phenomenon include the dispersive nature of bending waves and mechanical ringing or “reverberation”.

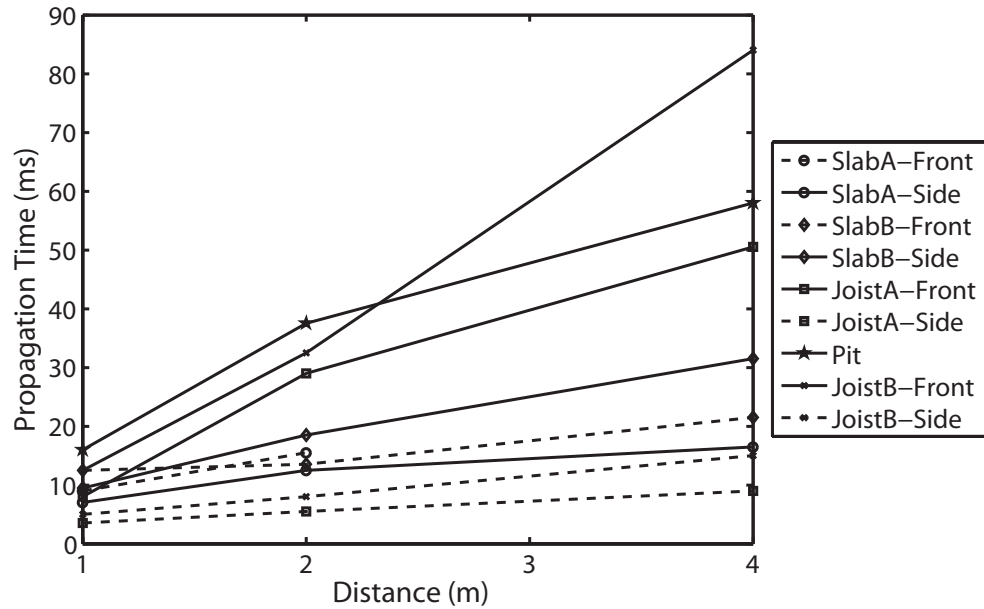


Figure 6.7: Vibration propagation times as a function of distance.

Also of interest is the propagation time between source and receiver. This value is calculated using the cross-correlation function as described in Section 5.1.2. Propagation times measured for each source/receiver combination are presented graphically in Figure 6.7 and in Appendix H. The resulting differences in arrival time between vibration and the audio signals traveling through air are also presented in Figure 6.8 and Appendix H.

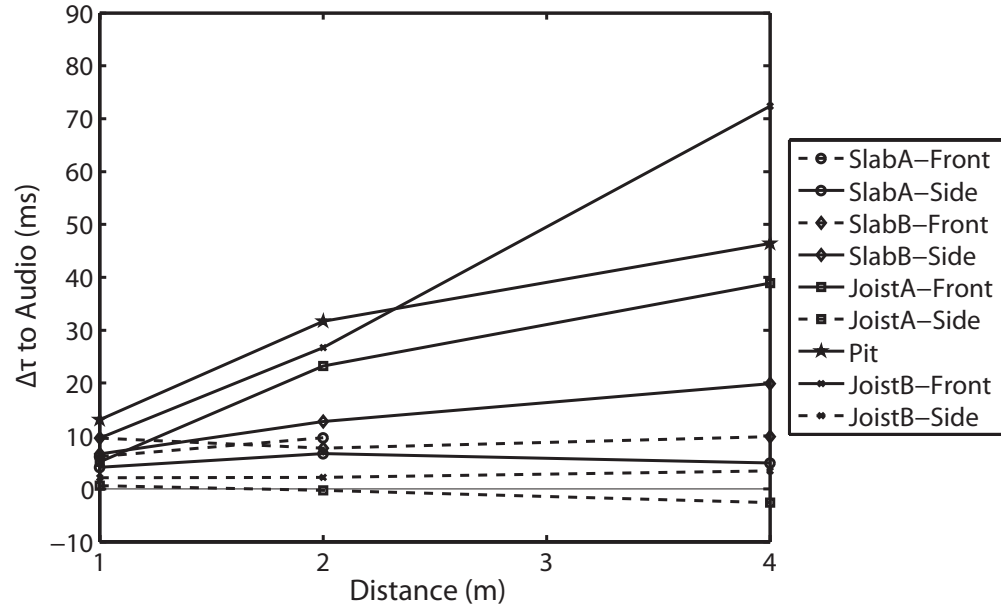


Figure 6.8: Time delay between vibration and audio signals as a function of distance.

6.2 Human Response

Ten individuals completed the subjective test as described in Section 5.3.2. Volunteer subjects varied in age between 23 and 38 years and were recruited via email or personal invitation. Eight of the subjects play a musical instrument and four have had formal training. Their responses resulted in ten difference matrices which are evaluated through multidimensional scaling. Each individual subjective response can be found in Appendix I. Two methods of MDS are used: two-way for an average matrix and three-way for individual difference scaling.

6.2.1 Multidimensional Scaling Configurations

6.2.1.1 Two-Way MDS

Averaging each value in the stimulus difference matrices results in the average difference matrix shown in Table 6.1.

Ordinal MDS with broken ties is used to create configurations of 5 different dimensionalities. The scree-plot in Figure 6.9 shows the expected improvement of fit with increasing dimensionality, but no apparent knee. Kruskal Stress-1 values

indicate a very good level of fit across all dimensionalities, well below the fit expected for a random data set.

The lack of a knee in the scree-plot provides no initial indication of the true dimensionality of the data set. A two-dimensional configuration is presented in Figure 6.10. Each data point represents a vibration signal experienced on an individual stage construction and the two axes represent some perceptual parameter or combination of parameters by which subjects rated the differences in vibration.

6.2.1.2 Individual Difference Scaling

Ordinal MDS with broken ties is also used for three-way, individual difference scaling. In this case, stimulus-space configurations are created for each subject using their individual difference matrices. A combined group stimulus space is evaluated in the same way as the two-way stimulus space. In addition, a subject space is also presented to examine the relative importance of each dimension to individual subjects.

Table 6.1: Difference matrix found by averaging subjective difference ratings across subjects.

	1	2	3	4	5	6	7	8	9	10	11	12	13	14
1	-	3.3	2.3	3	3.6	2.3	2.3	4.2	2.3	2.5	4.3	2.4	4.3	5.3
2	3.3	-	3.9	3.1	5.4	4.3	5.4	5.7	2.7	3.8	2.8	2.8	2.5	3.5
3	2.3	3.9	-	4.7	2.8	1.9	1.9	2.8	2.6	2.7	5.3	4	5.1	6.2
4	3	3.1	4.7	-	5	4.1	3.8	5.4	2.9	3.5	4.5	2	3.2	3.9
5	3.6	5.4	2.8	5	-	2.3	2.1	2.2	4.2	3.2	6.2	5.1	5.5	6.3
6	2.3	4.3	1.9	4.1	2.3	-	1.6	2.6	2.1	2.4	5.6	4.5	5.7	6
7	2.3	5.4	1.9	3.8	2.1	1.6	-	2.7	2.8	2.4	5.2	4	5	6.5
8	4.2	5.7	2.8	5.4	2.2	2.6	2.7	-	4.6	3.9	6	5.3	5.7	6.7
9	2.3	2.7	2.6	2.9	4.2	2.1	2.8	4.6	-	2.3	3.6	2.8	3.5	6
10	2.5	3.8	2.7	3.5	3.2	2.4	2.4	3.9	2.3	-	3.7	2.6	3.4	5
11	4.3	2.8	5.3	4.5	6.2	5.6	5.2	6	3.6	3.7	-	3	3.3	2.4
12	2.4	2.8	4	2	5.1	4.5	4	5.3	2.8	2.6	3	-	2.2	4
13	4.3	2.5	5.1	3.2	5.5	5.7	5	5.7	3.5	3.4	3.3	2.2	-	3.7
14	5.3	3.5	6.2	3.9	6.3	6	6.5	6.7	6	5	2.4	4	3.7	-

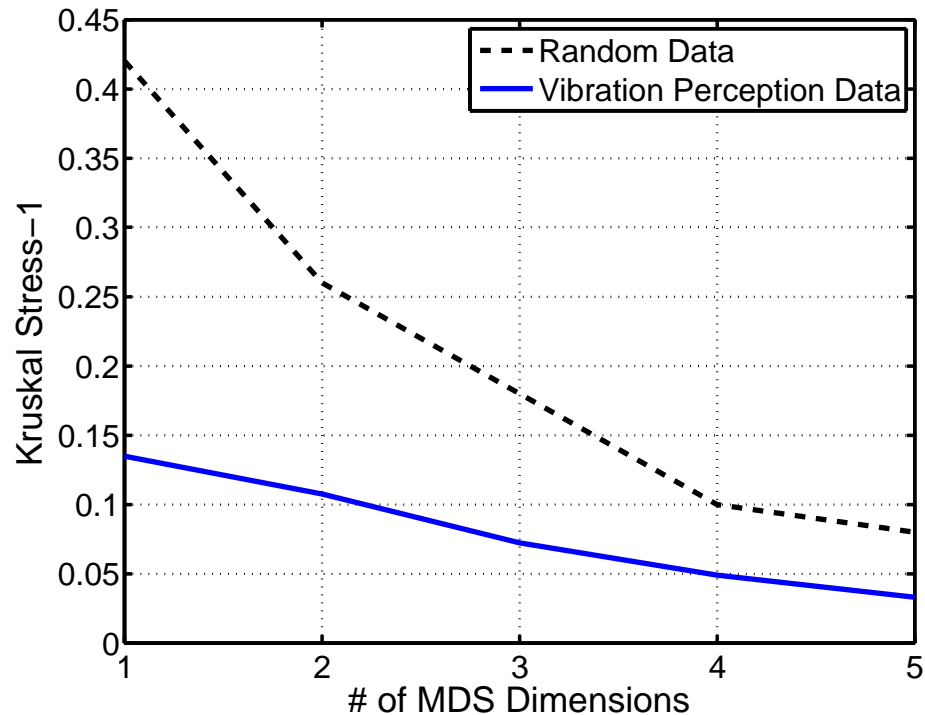


Figure 6.9: Kruskal Stress-1 values calculated for two-way MDS configurations of five dimensionalities. “Random Data” represents Stress-1 values for an equivalent MDS configuration generated with a set of random numbers as the input.

MDS configurations of five different dimensionalities are created in search of the best fit. The scree-plot in Figure 6.11 shows the Kruskal Stress-1 values of the group space found for each dimensionality.

Stress values for each individual difference scaling dimensionality are significantly higher than those found in the two-way case. The reason for this is that individual difference scaling attempts to account for differences in perception across individual subjects’ responses. The fairly abstract and unfamiliar nature of this experiment has likely resulted in large differences in individual perceptual “strategies” for ranking resulting in “noisy” data. However, because each subject has only ranked each set of stimuli once, there is no method of evaluating repeatability. As in the two-way case, there is no apparent point at which an increase in dimensionality stops improving the fit. However, stress values exceed the goodness-of-fit for a configuration modeling random noise at a dimensionality of approximately 3.

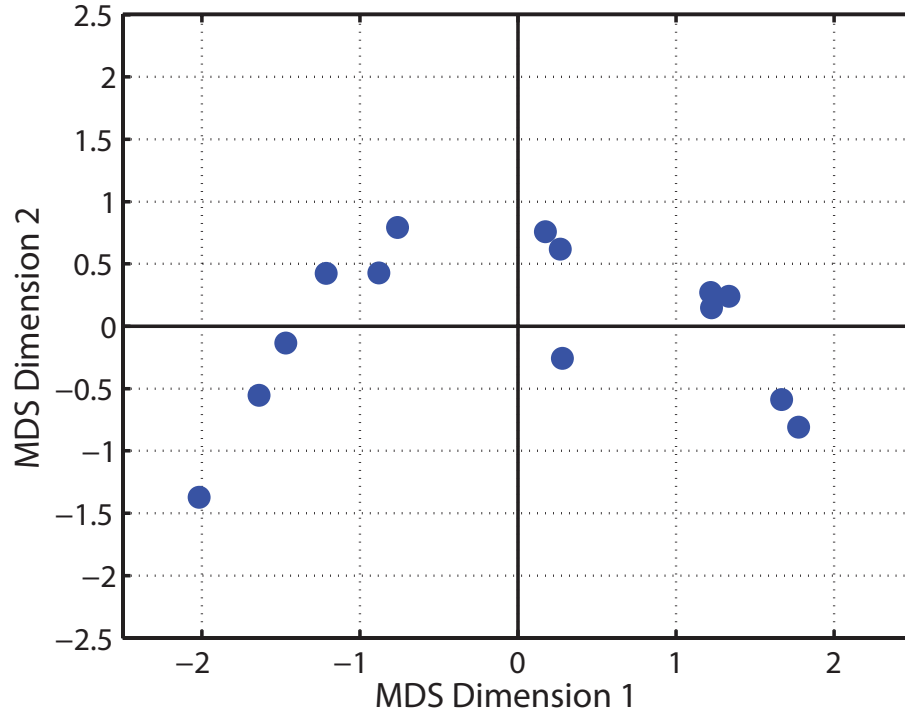


Figure 6.10: Two-dimensional, two-way MDS configuration. Each point represents a different stimulus.

Fit data presented in Figures 6.9 and 6.11 both apply to the same data and stimulus set and should therefore share the same core dimensionality. MDS stress exceeds that for a model fit to random data a dimensionality of 3 in the individual difference scaling procedure. As a result, it is unlikely that subjective differences measured in this test are made with more than two perceptual dimensions. The lack of a knee in either scree-plot supports this hypothesis. A two-dimensional, individual difference scaling MDS group stimulus space is shown in Figure 6.12 along with the associated subject space in Figure 6.13.

6.2.2 Correlation to Physical Parameters

One of the goals of this experiment is to find a connection between the perceptual dimensions identified through MDS with physical characteristics of the stimuli. Listeners are not required to rate specific physical properties during the subjective experiment. As a result, perceptual dimensions identified can be compared to any

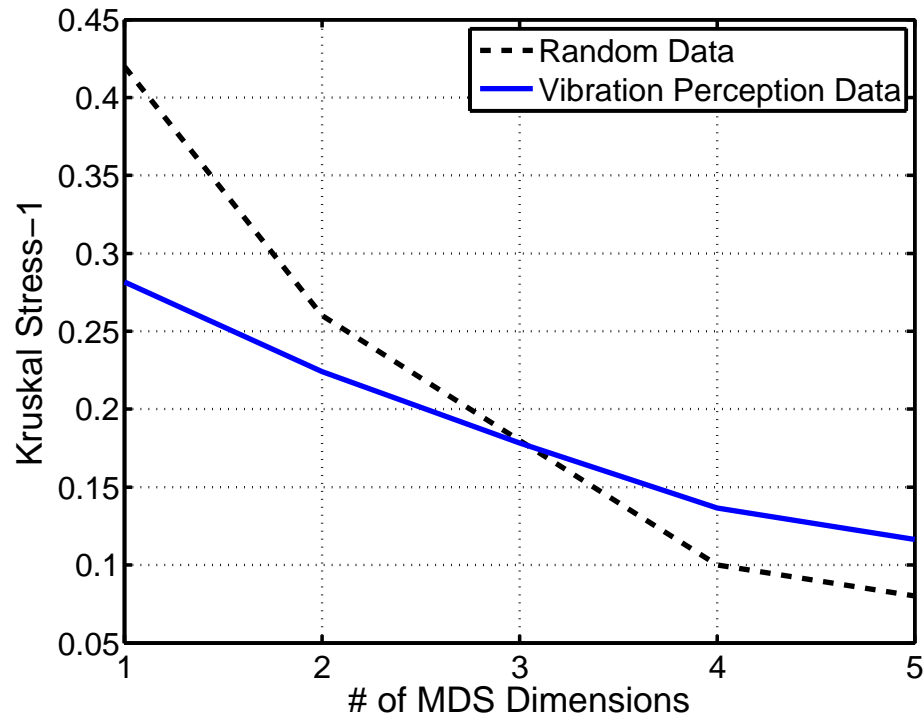


Figure 6.11: Kruskal Stress-1 values calculated for individual difference scaling MDS configurations of five dimensionalities. ‘Random Data’ represents Stress-1 values for an equivalent MDS configuration generated with a set of random numbers as the input.

physical parameter chosen by the experimenter. Eleven physical parameters are selected for evaluation with respect to the perceptual dimensions obtained through MDS. Each of the magnitude values are measured on the platform at the bottom of the seat with a 180 pound human subject are presented in Table 6.2.

The first seven values listed in Table 6.2 represent measures of sensation level, each responding differently to the stimulus’ frequency content or temporal attributes. The values reported are measured with a 180-lb subject sitting on the platform. Vibration levels would be higher for lighter subjects. The eighth value is the difference in arrival time between tactile and audio signals presented to the listener, with a negative value indicating a lead by vibration. The remaining three parameters are measures of frequency content independent of magnitude. The two ‘bass ratio’ values represent the ratio of energy below the crossover frequency to that above the crossover frequency. The spectral center of gravity is the frequency

Table 6.2: Physical parameters measured at the middle of the seat with a 180-lb human subject seated on the platform. %>thresh. = % of signal above human threshold for perception, W_k = frequency weighting, B.R. = bass ratio, Spec. CoG = spectral center of gravity.

Stim. #	%> thresh.	ms^{-2} r.m.s.	ms^{-2} r.m.q.	$W_k ms^{-2}$ r.m.s.	$W_k ms^{-2}$ r.m.q.	ms^{-1} r.m.s.	ms^{-1} r.m.q.	dT (ms)	B.R. 50Hz	B.R. 72Hz	Spec. CoG (Hz)
1	8.1	0.18	0.37	0.006	0.011	45.1	51.1	6.1	0.18	0.64	75
2	5.3	0.12	0.22	0.005	0.01	31.8	42.5	9.7	0.1	0.7	75
3	20.3	0.23	0.4	0.01	0.016	68	81.8	4.1	0.12	0.54	76
4	2.4	0.14	0.36	0.004	0.009	100.9	114	6.7	0.11	0.52	77
5	27.1	0.37	0.8	0.013	0.026	16.2	21.6	9.6	0.18	1.24	69
6	27.2	0.23	0.37	0.012	0.02	18.3	22	7.7	0.03	0.66	76
7	19	0.24	0.45	0.009	0.015	110.1	138.6	6.6	0.04	0.33	81
8	37.7	0.31	0.54	0.018	0.028	64.4	83.1	13.1	0.12	0.8	72
9	17.3	0.17	0.27	0.008	0.014	92.3	113.1	31.7	0.11	0.7	74
10	10.9	0.2	0.4	0.007	0.013	26	29.8	9.6	0.44	1.5	64
11	1.9	0.06	0.14	0.003	0.008	233	263.6	26.7	0.56	3.63	58
12	2.3	0.13	0.29	0.003	0.007	178.4	210.6	2.1	0.4	1	69
13	1.1	0.1	0.23	0.003	0.005	101.7	123.9	2.2	0.18	0.73	74
14	0.1	0.03	0.08	0.002	0.003	64.6	89.7	3.4	0.39	1.24	67

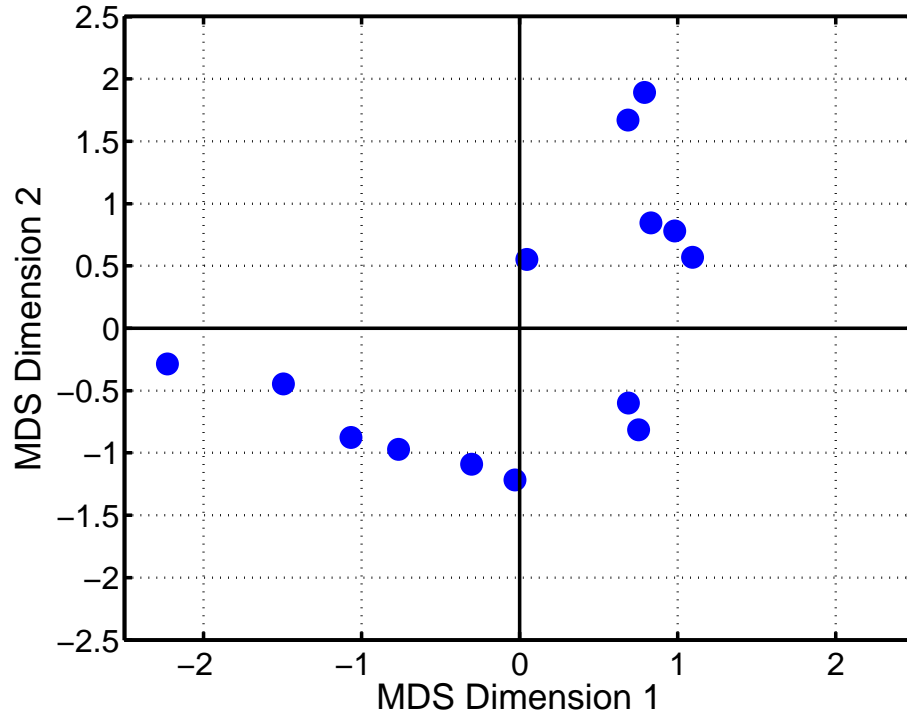


Figure 6.12: Two-dimensional, individual difference scaling MDS configuration. Each point represents a different stimulus.

for which equal energy exists above and below, within the valid frequency in this experiment of 30-100 Hz. Spectral measures are taken from the structural impulse responses rather than platform measurements for clarity.

Linear regression is used to identify correlations between the physical parameters shown in Table 6.2 and the axis of MDS configurations as discussed in Section 5.3.1.2. The Pearson product-moment correlation coefficients obtained from correlation of eleven parameters with the 1,2 and 3 dimensional two-way and individual difference MDS configurations are presented in Figures 6.14 through 6.16. Correlation coefficients can also be found in Tables J.1 and J.2 in Appendix J.

In some cases, definite trends in data sets can be identified simply by identifying similarities in groups of data points in close proximity to one another. Several plot labels taken from Table 6.2 are explored. When sensation levels are plotted as labels, the model shows not only a monotonic increase along the axis of highest correlation, but that sensation levels are quite close in groups. This grouping could

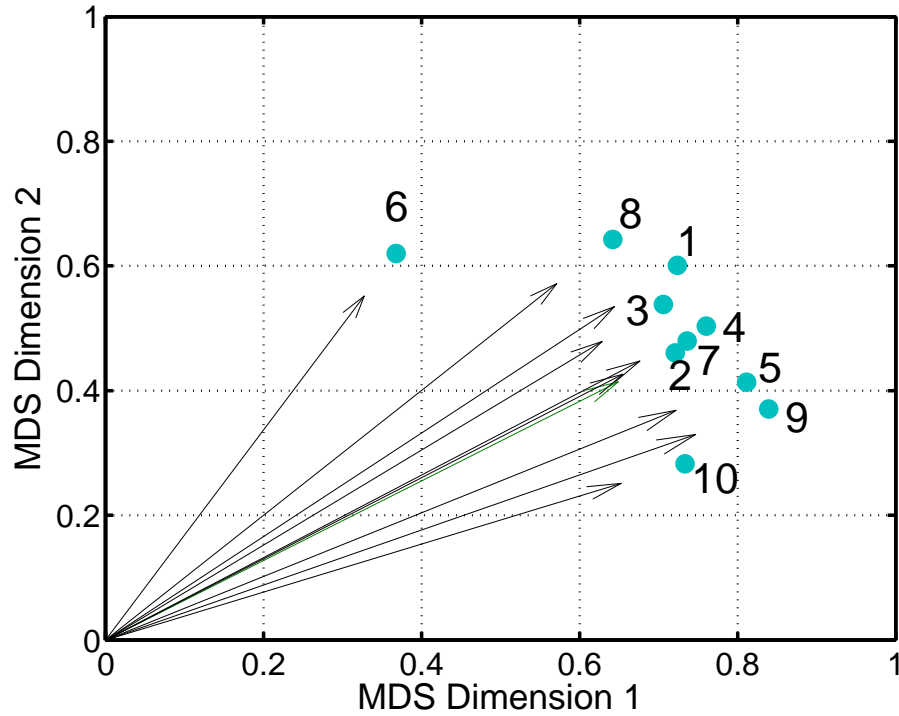


Figure 6.13: Two-dimensional subject space for individual difference scaling MDS configuration. Each vector represents a difference subject and the importance of each dimension used in making their difference ratings.

indicate that both of the axis are related to sensation level. Unweighted acceleration, the measure of sensation level with the highest correlation, is used to label and plot the two-way MDS configuration, shown in Figure 6.17.

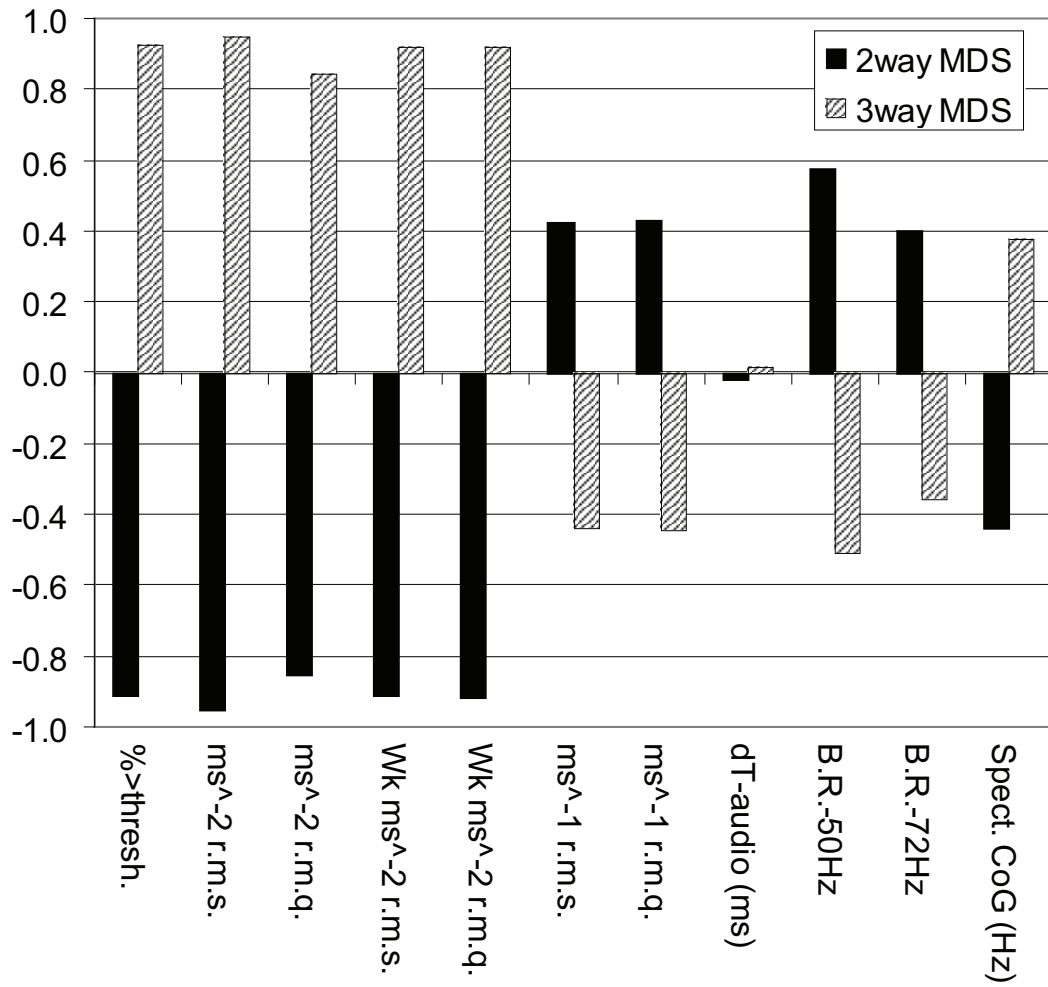


Figure 6.14: Coefficients of correlation between physical parameters and one-dimensional MDS configurations. 2 way configurations are shown by solid bars. 3 way configurations represent individual difference scaling models, and are shown in dashed bars.

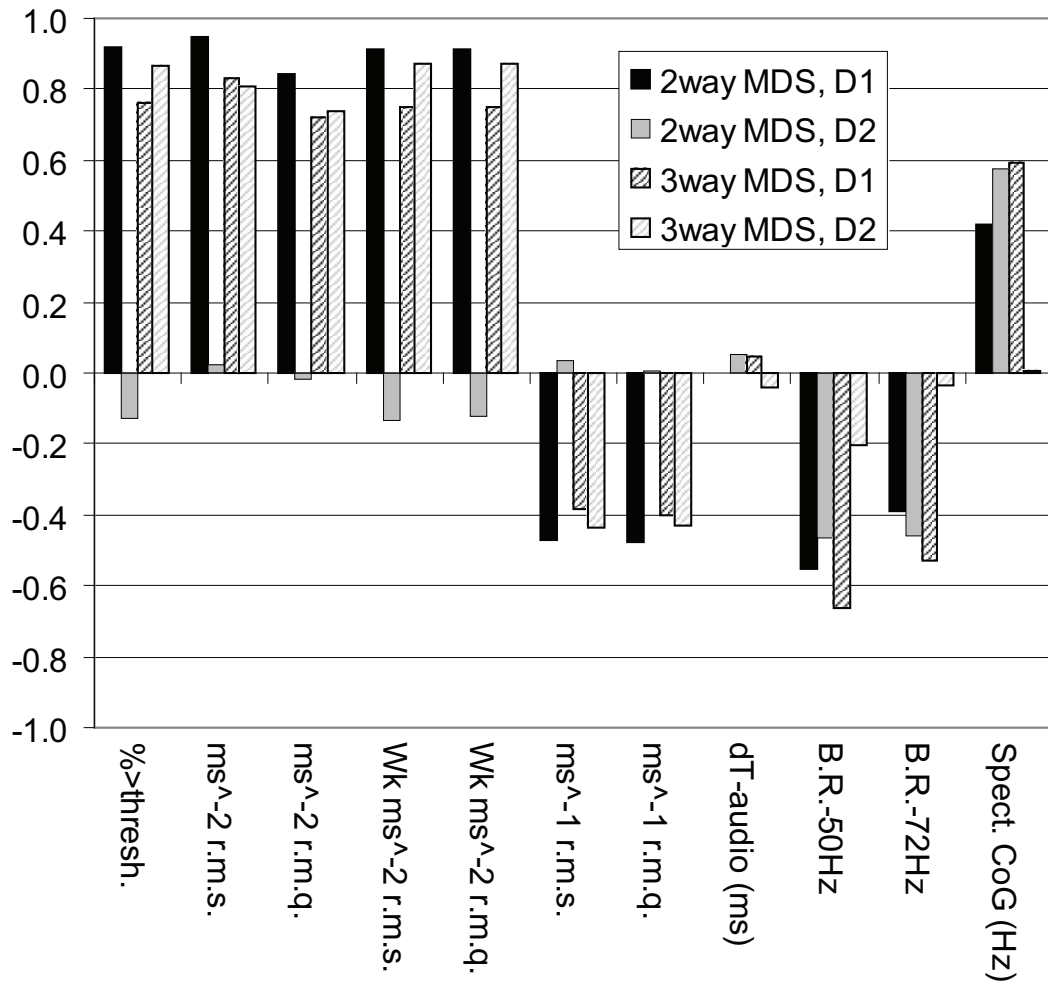


Figure 6.15: Coefficients of correlation between physical parameters and two-dimensional MDS configurations. 2 way configurations are shown by solid bars. 3 way configurations represent individual difference scaling models, and are shown in dashed bars.

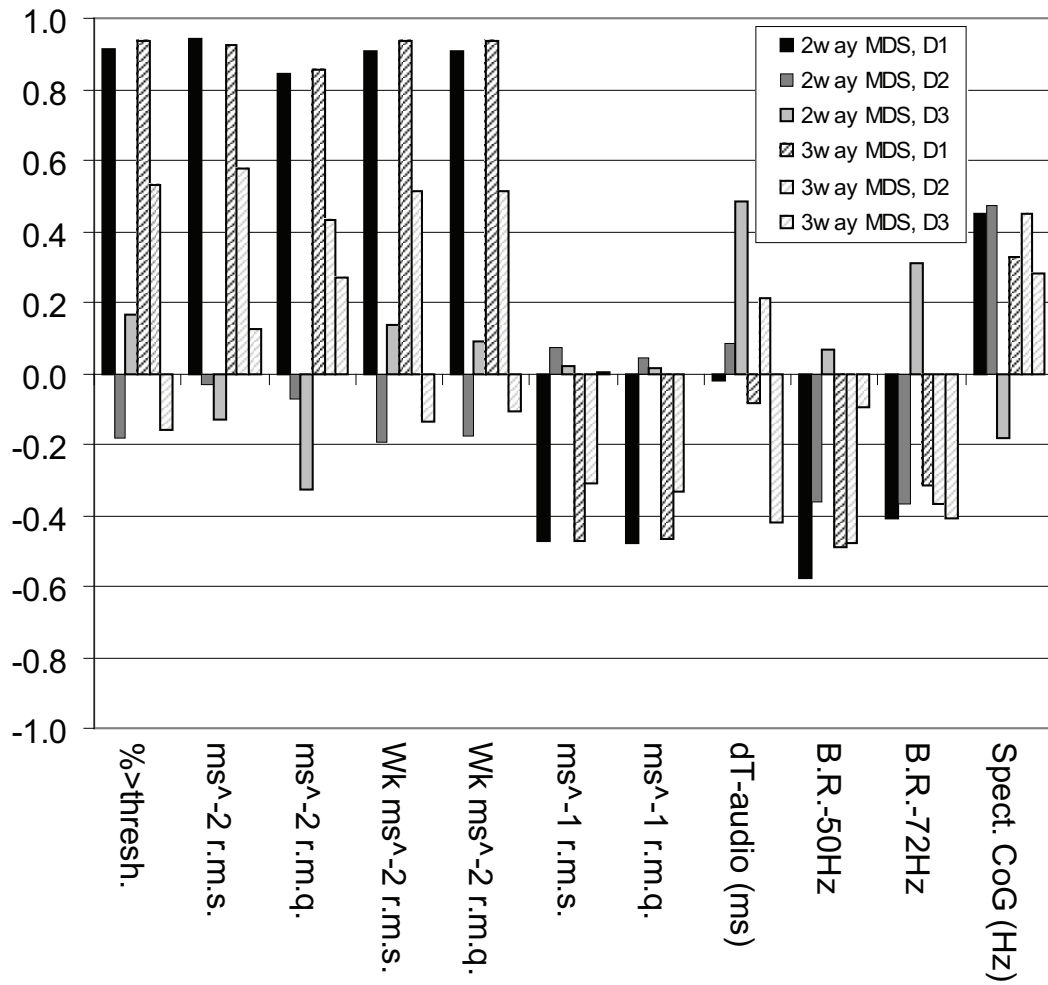


Figure 6.16: Coefficients of correlation between physical parameters and three-dimensional MDS configurations. 2 way configurations are shown by solid bars. 3 way configurations represent individual difference scaling models, and are shown in dashed bars.

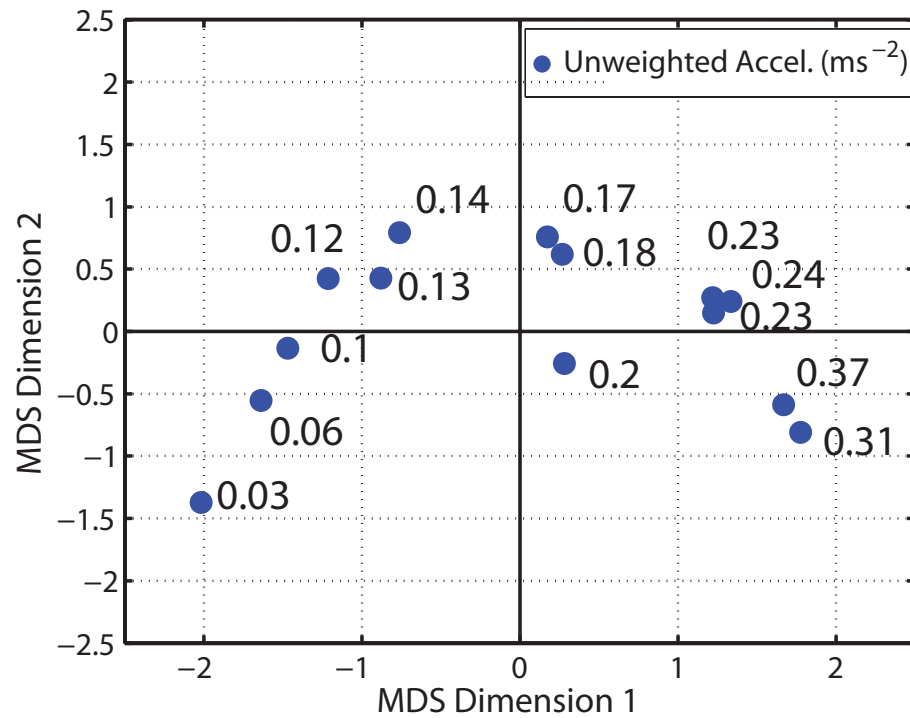


Figure 6.17: Two-dimensional, two-way MDS configuration. Each point represents structural vibration perceived on a different stage construction. Stimuli are labeled with unweighted acceleration measured on the platform.

6.2.3 Survey Responses

Subjects were provided with a short survey during debriefing. Each subject was asked to answer the following questions:

- Did the presentation seem realistic?
- Do you feel the presence of vibration added to the plausibility of the musical presentation?
- What strategy did you use to differentiate between signals?
- What characteristics of the vibration most heavily influenced your difference rating?
- Describe the vibration signals that you most preferred.

In response to this survey, 7 of the 10 subjects stated directly that they used intensity or sensation level to differentiate signals. Four of the subjects stated a difficulty in putting words to their method of differentiating signals. Other methods of differentiation mentioned are “different types of tingling sensations in different areas of my body”, “area of stimulation”, “highest frequency of vibration”, “frequencies that the stage responds to” and “directionality in the vibration signals”. One subject mentioned “quickest response to audio signal” in response to a question regarding preference. All 10 subjects stated that the presentation seemed realistic and added to the perception of presence.

7. Discussion

7.1 Structural Response

Structural impulse response measurements conducted in this study indicate a wide range of response magnitudes, both physical and perceptual. This was expected to some degree, due to the modal nature of wood floor constructions. Not expected was the lack of a clear trend separating concrete slab and wood floor constructions. The data presented in Figure 6.3 shows that of the stages responding with the highest magnitudes, one is the orchestra pit riser and the other a concrete slab stage. Following that, a group of similar magnitudes of vibration occur on a joisted stage and four concrete constructions, followed by two lower magnitudes on one of the joisted stages. The linear levels plotted in Figure 6.3 correspond more accurately to differences in perception than logarithmic levels, as discussed in Section 3.1.1.

The concrete slab stage exhibiting the highest magnitude happens to be supported by a by a Mason Industries jack-up spring system. The author expects the first resonant frequency designed for the system is much lower than the frequencies measured in this study, but the spring system could result in some compliance above this isolation frequency. However, the lower vibration magnitudes observed in the perpendicular direction from the receiver do not support this theory, showing similar response magnitudes to the other concrete slab stage measured.

Low magnitudes of response observed in the Joist-A stage are explained by the fact that the receiver position is inadvertently located directly above a major support beam, verified by visual inspection after the measurements are conducted. When measurements are conducted on the Joist-B stage, which is nearly identical in structure and floor covering, the receiver measurement position is chosen to be directly between two beams, also verified visually. The resulting magnitudes are observed to be much higher for all source locations. Support beams at the source location also affect vibration response, as shown by the two data points found to be much lower than the trend of vibration attenuation with distance observed when measurements are not conducted over a beam.

High correlation coefficients of linear regression to logarithmic levels of vibration with distance provide strong evidence for the wave-based model of propagation in stage structures. The observation of two statistically significant mean decay rates indicates that while modal response is present, it is not dominant, even in wood joisted constructions. The exception is that when source or receiver locations are positioned above support beams, vibration levels are reduced drastically.

Observation of structural response in the frequency domain indicates that narrow air space, close spacing of sleepers and stiffness in the two concrete slab constructions provide higher levels of damping than the open, wood floor constructions. Modal type frequency response may have implications for highlighting certain notes on an instrument coupled to the floor. In addition to the “modalness” of frequency response functions, slight variations in the balance of low to high energy between 10 and 100 Hz are observed (see Appendix G).

Propagation times appear to increase linearly with distance in Figure 6.7, indicating a constant speed of sound for each combination of stage construction and measurement direction. Changes in slope indicate varying speeds of sound dependent on both stage construction *and* direction of propagation. Positive slopes for each measurement set show that the speed of sound in most structures is slower than that of air (sound speed values can be found in Appendix H). Commonly accepted knowledge says that sound—which is typically analyzed in frequencies ranging up to thousands of Hertz—travels faster in solids than in air. However, these results highlight the frequency dependence of the speed of bending waves in solids, and show that at low frequencies, sound is observed to travel *slower* in solids than in air.

The results shown in Figure 6.8 indicate time delays between audio and vibration of up to 74 ms, with vibration lagging in nearly all cases. These results are interesting in light of the results presented by Daub and Altinsoy and Walker *et al.* Daub and Altinsoy found that subjects chose subjective points of audio-tactile simultaneity preceding the point of objective simultaneity for all listeners. Walker *et al.* also found PSS preceding POS for three instruments ranging from -30 ms to -2 ms and a PSS lagging POS for two instruments from 2 ms to 15 ms.

The question to be asked is then, why do humans perceive vibration to advance audio in subjective experiments when real-world musical conditions indicate that vibration more often than not lags audio? The answer may remain in the point at which we identify objective simultaneity. As discussed in Section 4.1, the vibration responsible for whole-body excitation travels in the form of dispersive waves. In these waves, high frequencies travel faster than low frequencies. Using the cross-correlation function to identify the point of objective simultaneity between audio and tactile signals simply selects the point of maximum amplitude as the arrival time for vibration, ignoring frequency information. It is possible that high frequency vibration is more important for the perception of temporal synchrony. If a high pass filter were applied to the structural impulse response, the cross-correlation function would indicate an earlier time of arrival which may coincide more with perceived temporal synchrony.

7.2 Human Response

The correlation coefficients between axes of MDS configurations and physical parameters presented in Figures 6.14 through 6.16 provide an important insight into how humans perceive differences in vibration signals. Physical parameters with high correlations are likely to influence the perception of differences while those with low correlation are likely to be relatively unimportant. Understanding the perception of differences is a prerequisite for understanding preference.

A look at the one dimensional models in Figure 6.14 shows strong correlation with all of the % -above-threshold or acceleration measures and weak correlation to the velocity and frequency parameters. The inverse signs of the two-way and individual difference scaling models indicate that the two configurations are very similar, but rotated by 180 degrees with respect to one another. High correlations between measures of sensation level also occur in the 2 and 3 dimensional models shown in Figures 6.15 and 6.16. Comparing the two-dimensional and three-dimensional models shows that a third axis provides very little correlation to any parameter for both two-way and individual difference MDS, which provides evidence that the true

dimensionality of perception in this study is two in addition to the fit data discussed in Section 6.2.

If the models are perceptually orthogonal, a parameter that is highly correlated with one axis should have a low correlation to all other axis. Orthogonality is observed to some degree only in sensation level measures for the 2-dimensional two-way model shown by the solid bars in Figure 6.15. The remaining frequency measures in the two-way MDS configuration and all parameters in the three-way MDS configuration show similar correlations to both axes, a lack of orthogonality.

It is possible that averaging all subjective responses into the two-way difference matrix normalized the importance of a two competing dimensions to zero. The individual difference subject space shown in Figure 6.13 shows that all subjects found both axes of perception to be important in discerning differences, with some subjects leaning more heavily towards the first axis. Correlation coefficients in Figure 6.15 show that both of these axis might be different perceptions of sensation level. When individual differences in perception are eliminated, the two axis of the three-way model might have collapsed into one important axis in the two-way model with the other representing only a fit to noise.

The hypothesis that both the axes in the 2-dimensional configurations represent some frequency dependent measure of sensation level is supported by the configuration itself, shown in Figure 6.17. Even in the two-way model, groupings of stimuli seem to be controlled by the sensation level measure with the highest correlation coefficient: unweighted r.m.s. acceleration. Small differences in acceleration create tight groups of stimuli using *both* axis.

Sensation level measures show stronger correlation than any of the temporal or frequency measures. In fact, correlation to the time difference between tactile and audio signals is extremely low across all configurations. This low correlation indicates that audio-tactile time delays are relatively unimportant in evaluating differences in tactile signals in a multimodal environment. Previous studies have reported a strong ability to identify audio-tactile time delays with unexplained variation with musical instrument. The results of this study do not refute these findings, but show that when asked to evaluate signals in their natural form, audio-tactile

time delays are swamped by differences in magnitude. Results of the studies by Daub/Altinsoy and Walker *et al.* indicate that humans have the ability to judge audio-tactile synchrony, but do not draw conclusions regarding the importance of synchrony in perception of musical situations.

The variety of sound speeds measured in structures indicates that there may be some ecological basis for the relative unimportance of audio-tactile time delays. In other modes of perception such as the audio-visual relationship, differences in arrival time of information change have a clear relationship. The small variation of the speed of sound in air and the constant speed of light means that time delays at a given distance will remain constant across nearly all situations experienced in normal life. In the audio-tactile relationship, the time delay relationship between modes of perception is observed to change with floor construction and even position on a floor. The constant fluctuation of tactile propagation times means that humans do not get the chance to build up a reference upon which to compare tactile signals.

A strong correlation between perceptual differences and sensation level in vibration is not surprising. The auditory equivalent “loudness” has long been understood to govern perceived differences and even preference in sonic environments. As a result, auditory stimuli are adjusted to have equal loudness in modern studies in order to amplify other perceptual differences, as in the studies conducted by Grey and Schroeder, Gottlob and Siebrasse [16], [32]. Differences in sensation level were included in Yamaguchi’s study using MDS to explore differences in concert hall sound fields [35]. Yamaguchi used loudness to “calibrate” the orientation of the MDS configuration such that one axis had the highest correlation with sound pressure level. The problem with this approach is that researchers have found that in MDS studies, the inclusion of one very strong perceptual difference can overpower other differences [31]. Other would-be dimensions in the MDS configurations get flattened into one and represent a fit to other aspects of the first dimension noise.

The inclusion of different magnitudes of vibration in this study has (1) identified sensation level as the dominant physical parameter in perceptual differences and (2) suppressed the ability to identify the importance of other physical parameters. The most highly correlated measure of sensation level in all MDS configura-

tions is unweighted r.m.s. acceleration. This finding supports the results reported by Howarth and Griffin that humans may be more sensitive to high frequency vibration than indicated by the ISO 2631 frequency weighting contour, especially in critical listening situations such as music performance [20]. While other perceptual differences are suppressed, the results show that time synchrony of audio and tactile signals and frequency characteristics are at least not as important as sensation level.

The large number of subjects identifying sensation level as a strategy of differentiation supports the findings of the MDS metrics while other responses provide some indication of other parameters that are harder to identify. The presence of only one listener commented regarding audio-tactile delay also verifies the lack of a correlation between this parameter and MDS configurations.

8. Summary and Conclusions

The results presented in this study have provided new information on the presence of vibration in stage constructions and the way in which humans perceived these vibrations. The findings are summarized as answers to questions posed at the beginning of this thesis.

How important is vibration in the perception of a musical performance?

All 10 subjects who completed the perceptual experiment stated that the presence of vibration made the musical performance seem more realistic and plausible. The positive response is verified by the measurement of vibration levels well above the threshold of human perception generated during the performance of a contrabass. The feeling of realism in a virtual presentation indicates that the memory of musical performances the subjects have experienced includes the tactile mode of perception. As a result, vibration in musical performances is an important part of the perception.

How do the materials and technique by which a stage is constructed affect vibration generated by musical performance?

Vibration is observed to propagate as a dispersive wave across stage platforms, resulting in predictably lower levels with distance. Structural beams are found to restrict this wave propagation, resulting in locations of low vibration either sources or receivers are positioned above them. Propagation time is found to vary with stage construction and orientation of path between source and receiver and beam lines. Audio-tactile time delays of up to 74 ms are observed with vibration most often lagging audio.

No methodical link is observed between the type of structure or finish material used and the overall magnitude of vibrational response. However, a wide range of physical magnitudes are observed, spanning the semantic labels of perception from “probably perceptible” to “very strong perception” dependent on listening position

and stage type. Structure and finish material are found to affect the amount of damping provided by a structure, with concrete slab constructions resulting in a smoother frequency response than joisted wood constructions or hydraulic risers.

What physical characteristics of musical vibration control human perception?

Physical magnitude dominates the perception of differences between vibration signals in an audio-tactile display. Frequency characteristics probably have some effect, but results are currently inconclusive. Time differences between audio and tactile signals are found to be insignificant as a result of the wide variety of vibration propagation times observed in real life situations compared to the relatively small variation of the speed of sound in air.

What requirements must be met to accurately represent the tactile mode of perception in a virtual display?

While differences in tactile signals generated on real stage constructions is controlled by sensation level, the impact of varying these levels on plausibility is most likely small. Only one subject provided a stipulation on plausibility by stating the presentation was plausible “in general, but not when it seemed way too strong.” The rule of thumb could be suggested that vibration magnitudes presented in a virtual display should be adjusted to be slightly above the threshold of perception so as to not draw attention by sensation levels that are too high.

The variety of magnitudes and frequency content measured on real stage constructions means that a wide range of presentation levels will be perceptually accepted. The relative insignificance of audio-tactile time delays indicates that audio-tactile synchrony is of low importance with respect to plausibility. However, the complex nature of dispersive wave propagation and variation of propagation times implies that tactile signals used in future investigation of audio-tactile synchrony must include measured vibration signals and a new method of identifying objective simultaneity. Finally, the subtle differences observed in structural frequency response and an indication of the perceptual importance of frequency information means that tactile displays must be calibration in the frequency domain.

LITERATURE CITED

- [1] BS 6841:1987 guide to measurement and evaluation of human exposure to whole-body mechanical vibration and repeated shock, 1987.
- [2] ISO 2631-1 mechanical vibration and shock - evaluation of human exposure to whole-body vibration - part 1: General requirements, 1997.
- [3] ISO 2631-2 mechanical vibration and shock - evaluation of human exposure to whole-body vibration - part 2: Vibration in buildings (1 hz to 80 hz), 1997.
- [4] M. Barron. The subjective effects of first reflections in concert halls - the need for lateral reflections. *J. Sound Vib.*, 15(4):475–494, 1971.
- [5] D. R. Begault. Auditory and non-auditory factors that potentially influence virtual acoustic imagery. In *Proc. Audio Engineering Society 16th International Conference*, Rovaniemi, Finland, April 10-12, 1999.
- [6] J. Blauert. *Spatial Hearing*. MIT Press, Cambridge, MA, 1997.
- [7] J. Blauert, H. Lehnert, J. Sahrhage, and H. Strauss. An interactive virtual-environment generator for psychoacoustic research. i: Architecture and implementation. *ACUSTICA/ACTA ACOUSTICA*, 86(1):94–102, 2000.
- [8] I. Borg and P. Groenen. *Modern Multidimensional Scaling: Theory and Applications*. Springer-Verlag, New York, 1997.
- [9] J. Braasch, D. Valente, and N. Peters. Sharing acoustic spaces of telepresence using virtual microphone control. In *Convention of the Audio Eng. Soc.*, New York, October 2007.
- [10] M. Daub and M. E. Altinsoy. Audiotactile simultaneity perception of musical-produced whole-body vibrations. In *CFA/DAGA '04 (Congrs Joint / Joint Congress 7me Congrès Français d'Acoustique CFA / 30th German Annual Meeting for Acoustics DAGA)*, Strasbourg, France, 2004.

- [11] D.J. Ewins. *Modal Testing: Theory and Practice*. Research Studies Press, 1986.
- [12] F. Fahy and P. Gardonio. *Sound and Structural Vibration: Radiation, Transmission and Response*. Academic Press, Oxford, UK, 2007.
- [13] A. C. Gade. Investigations of musicians room acoustic conditions in concert halls. part 1: Method and laboratory experiments. *Acustica*, 69:193–203, 1989.
- [14] A. C. Gade. Investigations of musicians room acoustic conditions in concert halls. part 2: Field experiments and synthesis of results. *Acustica*, 69:249–262, 1989.
- [15] A.C. Gade. Practical aspects of room acoustic condition measurements on orchestra platforms. In *14th International Congress on Acoustics Proceedings*, Beijing, China, 1992.
- [16] J. M. Grey. Multidimensional perceptual scaling of musical timbres. *J. Acoust. Soc. Am.*, 61(5):1270–1277, May 1977.
- [17] M. J. Griffin and E. M. Whitman. Discomfort produced by impulsive whole-body vibration. *J. Acoust. Soc. Am.*, 68(5):1277–1284, Nov. 1980.
- [18] M.J. Griffin. *Handbook of Human Vibration*. Elsevier Academic Press, 1990.
- [19] HEAD Acoustics, <http://www.head-acoustics.de> accessed on June 22, 2009. *Binaural Measurement, Analysis and Playback*, September 2006.
- [20] H. V.C. Howarth and M. J. Griffin. The frequency dependence of subjective reaction to vertical and horizontal whole-body vibration at low magnitudes. *J. Acoust. Soc. Am.*, 83(4):1406–1413, April 1988.
- [21] J. K. and C. W. Mueller. *Factor Analysis: What It Is and How to Do It*. Sage Publications, California, 1978.
- [22] J. B. Kruskal and M. Wish. *Multidimensional Scaling: Sage University Paper series on Quantitative Applications in the Social Sciences, 07-011*. Sage University Papers, 1978.

- [23] K. Walker, W. L. Martens, and S. Kim. Perception of simultaneity and detection of asynchrony between audio and structural vibration in multimodal music reproduction. In *Proc. Audio Engineering Society 120th Convention*, Paris, France, May 20-30, 2006.
- [24] P. Larsson, D. Västfjäll, and M. Kleiner. Ecological acoustics and the multi-modal perception of rooms: real and unreal experiences of auditory-visual virtual environments. In *Proceedings of the 2001 International Conference on Auditory Display, Epoo, Finland*, pages 245–259, 2001.
- [25] N. J. Mansfield and S. Maeda. Equal sensation curves for whole-body vibration expressed as a function of driving force. *J. Acoust. Soc. Am.*, 117(6):3853–8859, June 2005.
- [26] A. H. Marshall, D. Gottlob, and H. Alrutz. Acoustical conditions preferred for ensemble. *J. Acoust. Soc. Am.*, 64(5):1437, November 1978.
- [27] J. R. McKay. *Human perception of whole body vibration: some studies of perception and startle*. PhD thesis, University of Southampton, 1972.
- [28] T. Miwa. Evaluation methods for vibration effect part 7. the vibration greatness of pulses. *Ind. Health*, 6:143–164, 1968.
- [29] M. Morioka and M. J. Griffin. Difference thresholds for intensity perception of whole-body vertical vibration: Effect of frequency and magnitude. *J. Acoust. Soc. Am.*, 107(1):620–624, January 2000.
- [30] T. Rossing. *Personal communication at the Acoustical Society of America Conference in Portland, OR*. 18 May 2009.
- [31] S. S. Schiffman, M. L. Reynolds, and F. W. Young. *Introduction to Multidimensional Scaling*. Academic Press, New York, 1981.
- [32] M. R. Schroeder, D. Gottlob, and K. F. Siebrasse. Comparative study of european concert halls: correlation of subjective preference with geometric and acoustic parameters. *J. Acoust. Soc. Am.*, 56(4):1195–1201, October 1974.

- [33] I. Spence and D. W. Domoney. Single subject incomplete designs for nonmetric multidimensional scaling. *Psychometrika*, 39(4):469–490, December 1974.
- [34] K. A. Stetson. Singers’ preferences for acoustical characteristics of concert halls. Master’s thesis, Rensselaer Polytechnic Institute, Troy, New York, August 2008.
- [35] K. Yamaguchi. Multivariate analysis of subjective and physical measures of hall acoustics. *J. Acoust. Soc. Am.*, 52(5):1271–1279, 1972.
- [36] C. W. Yuen. Investigation of voice stage support: Subjective preference test using an auralization system for self-voice. Master’s thesis, Rensselaer Polytechnic Institute, Troy, New York, July 2007.

APPENDIX A

Mathematical Symbols

- α receptance (displacement/unit force)
- A accelerance (acceleration/unit force)
- a acceleration
- c wave speed / speed of sound
- $\Delta\tau$ audio-tactile time delay
- d_{ij} Euclidian distance
- e_{ij} error
- η displacement
- η_r damping loss factor
- E Young's Modulus
- f structural force *or* mathematical transformation
- FFT fast fourier transform
- H hysteric/structural damping
- I subjective intensity *or* second moment area of the cross section of the neutral axis of a bar
- K apparent stiffness
- k mathematical constant *or* wave number
- λ_r eigenvalues of hysterically damped structural system
- M apparent mass
- m mass per unit length
- N degrees of freedom
- n growth exponent
- p Pearson's product moment coefficient of correlation
- p_{ij} perceptual distance / disparity
- ϕ eigenvector of hysterically damped structural system
- ψ sensation level
- ψ_r eigenvector of hysterically damped structural system

σ_1 Kruskal Stress-1

R^2 coefficient of regression

r.m.s. root mean square averaging method

r.m.q. root mean quad averaging method

T/t time

ϑ physical magnitude

ω frequency

ω_r resonant frequency of hysterically damped structural system

X m-dimensional coordinate in MDS configuration

x distance

Y mobility (velocity/unit force)

APPENDIX B

Confounding Factors in the Perception of Vibration

From Handbook of Human Vibration [18]

Vibration characteristics

Type (sine, random, real)

Magnitude (r.m.s., peak. Vibration Dose Value, amplitude distribution)

Frequency (range, spectra)

Direction (axis, roll, pitch, yaw)

Input position (ischial tuberosities, back, feet)

Duration (each motion, total, rest periods)

Distortions (acceleration waveform distortion, background vibration, cross-axis motions)

Source (hydraulic vibrator, vehicle type, seat position and operating conditions)

Measurement method (accelerometers, signal conditioning, type and performance)

Other environmental conditions

Noise (level, spectra, correlation with vibration)

Lighting (illumination level, dark adaptation, viewing distance)

Thermal environment (temperature, humidity, airflow)

Seating or standing conditions

Seat type (real, simulated, experimental laboratory seat)

Seat components (squab, backrest, headrest, feet: position and orientation)

Seat dynamics

Harness

Position of seat (on vibrator, in vibrating room, in vehicle)

Orientation (standing, sitting, recumbent)

Posture (erect, slouched, uncontrolled)

Activities

Task description (principles, objective)

Information input characteristics (display size, position)

Information output characteristics (control position, control gain, control dynamics)

Instructions (objectives, motivation)

Performance measures (accuracy and speed)

Training (previous experience, learning effect)

Subjective assessments

Psychophysical method (rating, paired comparison)

Instructions (requirements of subject, set)

Subject training

Subject characteristics

Number of subjects

Type of subject (pilots, truck drivers, students, researchers)

Gender

Age

Dimensions of body (height, leg length, hip circumference)

Mass of body (weight, moments of inertia)

Posture

Experience (vibration, relevant tasks)

Expectation

Physical conditions (fitness, health)

Personality of subjects (introvert, extrovert)

APPENDIX C
Stage Construction Details and Structural Response
Measurement Positions

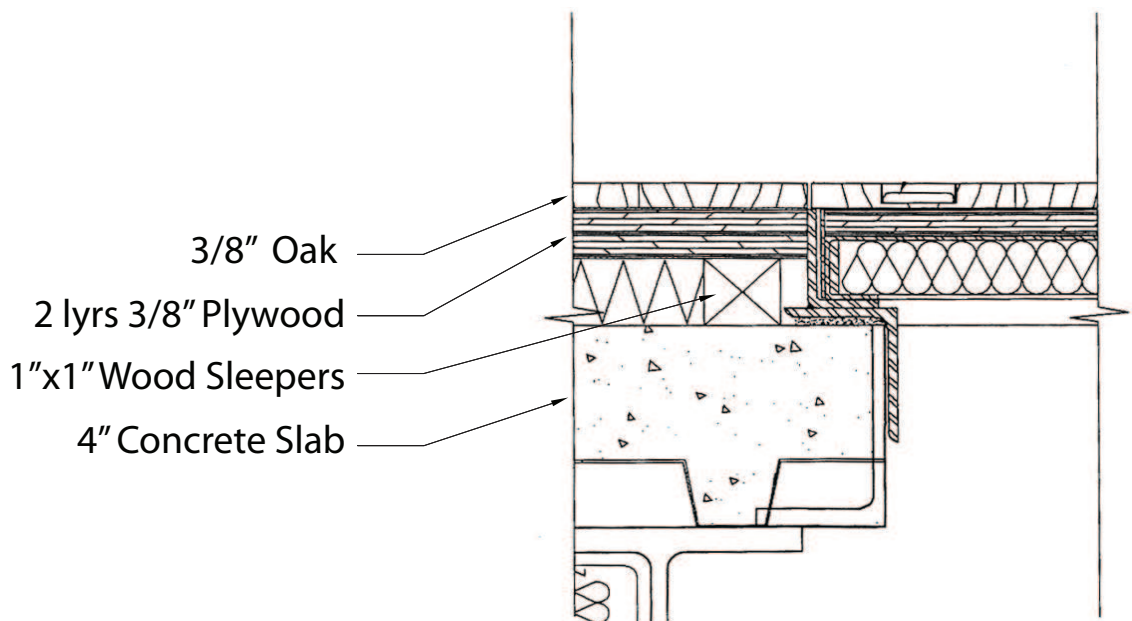


Figure C.1: Stage Construction Slab-A.

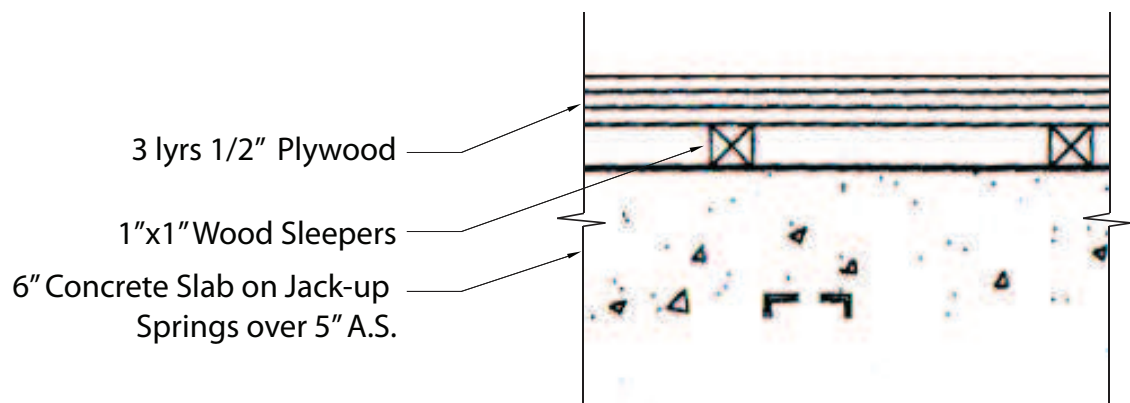


Figure C.2: Stage Construction Slab-B.

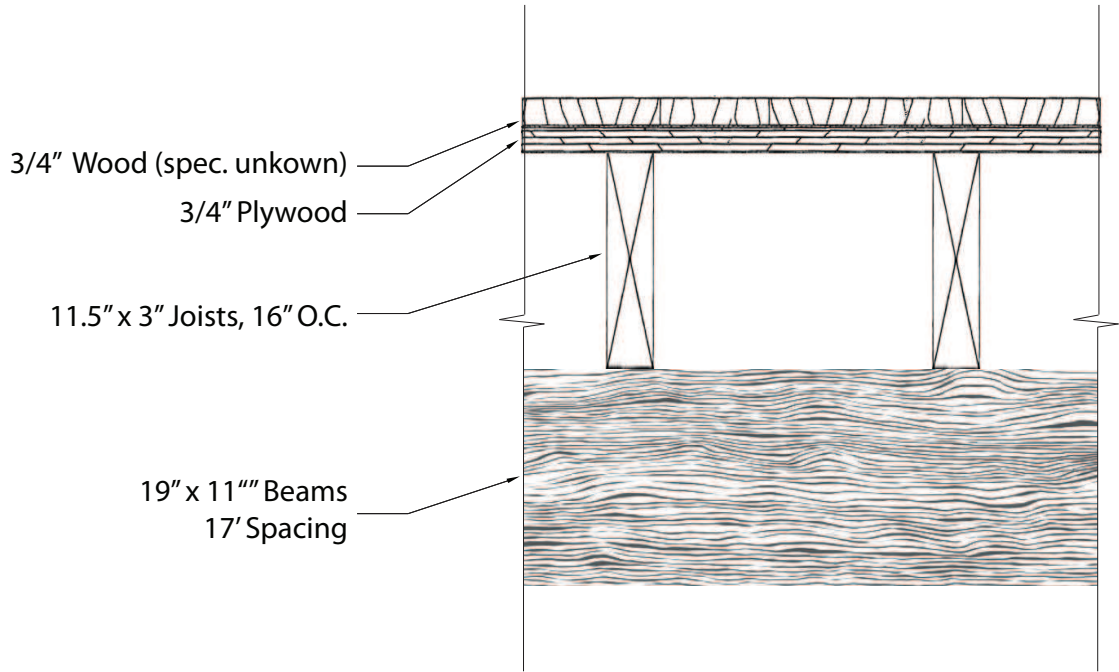


Figure C.3: Stage Construction Joist-A.

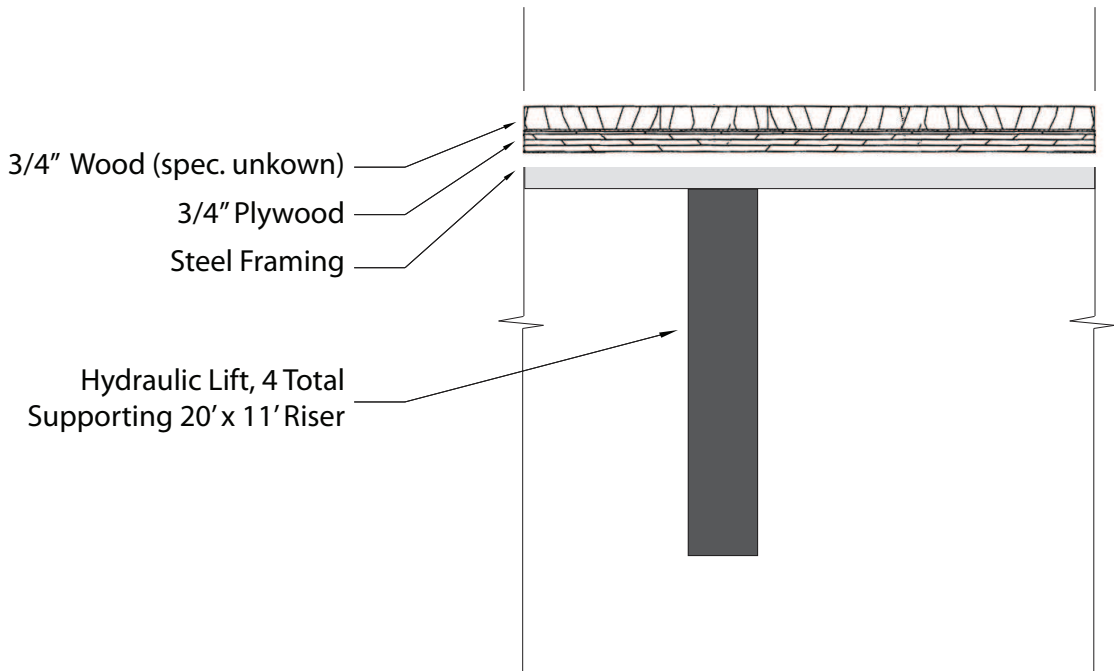


Figure C.4: Stage Construction Orchestra Pit Riser.

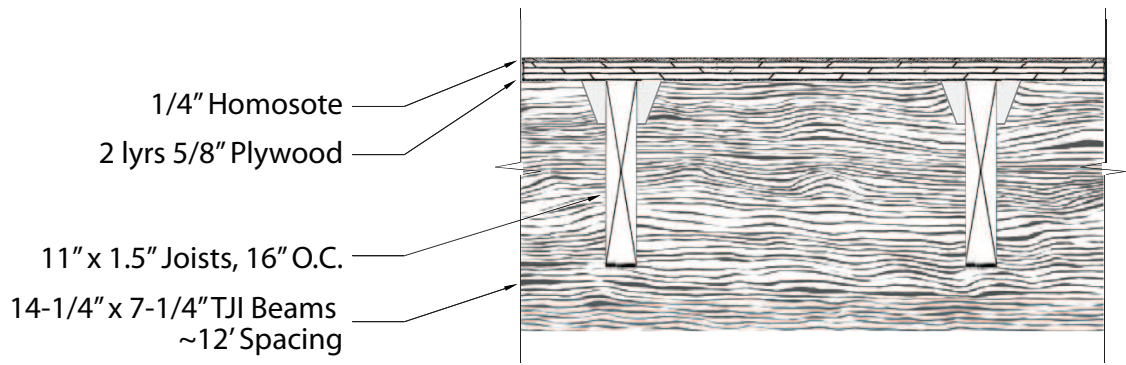


Figure C.5: Stage Construction Joist-B.

APPENDIX D
Institutional Review Board Approved Informed Consent
Form



INFORMED CONSENT FORM

The Architectural Acoustics program at Rensselaer Polytechnic Institute is conducting a study to explore the dimensions of perception of musical vibration. The study is conducted by asking participants to rate the similarity of vibration signals. Specific knowledge of music, acoustics, or vibration is not required to participate in this study.

Instructions for participant:

You are asked to judge how different a number of vibrations are. A short musical passage will be played through headphones while you are seated on a motion platform. During the experiment, you will be able to switch between two vibrations. Please rate the difference between the vibrations on a scale from 1-7 and continue on to the next set. If you find two vibrations completely different, rank them as “7”. If the two signals are identical, rank them as “1”. For all other cases, rank the signals somewhere in between according to your perceived difference. The sound heard through the headphones will be the same throughout the entire experiment.

The experiment will begin with a few sets of vibrations that will not be recorded. Please use these orientation tasks to orient yourself with the sounds and vibrations. The aim of this test is not to evaluate your individual performance, but to gather findings about the perception of vibration in general. Everyone’s perception is different and there are no “right” or “wrong” answers. Please make use of the entire difference scale and try to maintain a consistent method of ranking.

Please take your time to respond carefully to each presentation. Session length is determined in part by the participant and will not exceed a maximum duration of 30 minutes each for three sessions. You are encouraged to take a break during the experiment, and to end the session if you become fatigued with the option to continue at a later date. It is your right to discontinue participation at any point during the experiment without providing a reason. Any questions or reports of discomfort should be directed to the researcher.

Disclosure:

Sound pressure levels during the test will not exceed federal standards set by the Occupational Safety and Health Administration. Vibration amplitudes will not exceed the “health guidance zone” level identified in ISO 2631-1:1997(E) Annex B.

Your name will not be disclosed at any time. In oral and written presentations of this study, your responses will be assigned a number and will be grouped with those of the other participants for later analysis. Note that the results from this experiment will be held strictly confidential, and will in no way be associated with any individual participant.

I have read the above description and understand that I may discontinue participation at any point during the experiment without penalty. I also understand that my name will not be disclosed at any time before, during, or after the experiment. I have had the study explained to me, and have been provided an opportunity to have questions about the

NOTE: Do not sign this consent form if it does not have an IRB approval stamp, or if the date has lapsed.

study answered. I consent to participate in this study.

Signature: _____

Name: _____

Date: _____

For further information contact:

Clemeth L. Abercrombie, Architectural Acoustics Program, Rensselaer Polytechnic Institute
217.417.5657, abercc@rpi.edu

OR


Ted Krueger, Associate Prof., Rensselaer Polytechnic Institute
518.276.2562, krueger@rpi.edu

Institutional Review Board
Attn: Joelle Willis
Office of Research, CII 7015
Rensselaer Polytechnic Institute
110 8th Street
Troy, NY 12180
Telephone: 518.276.4232
Fax: 518.276.4002
Email: Telephone: 518.276.4232

NOTE: Do not sign this consent form if it does not have an IRB approval stamp, or if the date has lapsed.



APPENDIX E
Measurement Equipment Specifications

 PCB[®] PIEZOTRONICS	SPECIFICATIONS VOLTAGE OUTPUT ACCELEROMETER		REVISIONS -H- REV # 3004 DGM 11/13/90
			SHEET 1 OF 1
	MODEL NO.	308B	308B03
DYNAMIC			
Range ($\pm 5V$ output)	$\pm g$ (m/s^2)	50 (491)	100 (981)
Resolution	g (m/s^2)	0.001 (0.01)	0.002 (0.02)
Useful Overrange	g (m/s^2)	100 (981)	200 (1960)
Sensitivity ($\pm 2\%$)	mV/g ($mV/[m/s^2]$)	100 (10.2)	50 (5)
Frequency Range ($\pm 5\%$)	Hz	1-3000	1-3000
Frequency Range ($\pm 10\%$)	Hz	0.7-6000	0.7-6000
Transverse Sensitivity	%	≤ 5	≤ 5
Strain Sensitivity	$g/\mu\epsilon$ ($[m/s^2]/\mu\epsilon$)	0.05 (0.49)	0.05 (0.49)
Resonant Frequency [2]	kHz	≥ 25	≥ 25
Amplitude Non-Linearity [1]	% FS	≤ 1	≤ 1
Overload Recovery	μs	≤ 10	≤ 10
ELECTRICAL			
Excitation [3]			
Constant Current	mA	2-20	2-20
Voltage	VDC	24-27	24-27
Output Impedance	ohm	< 100	< 100
Output Bias	+volt	8 to 14	8 to 14
Ground Isolation		No	No
Discharge Time Constant (@R.T.)	s	≥ 0.5	≥ 0.5
Polarity		Positive	Positive
ENVIRONMENTAL			
Vibration (max)	g 's (m/s^2) peak	500 (4905)	1000 (9810)
Shock (max)	g (m/s^2)	5000 (49050)	10000 (98100)
Temperature Range	$^{\circ}F$ ($^{\circ}C$)	-100 to +250 (-73 to +121)	-100 to +250 (-73 to +121)
Temperature Coefficient	$\%/^{\circ}F$ ($\%/^{\circ}C$)	≤ 0.03 (0.05)	≤ 0.03 (0.05)
PHYSICAL			
Structure		Upright	Upright
Size: hex x height	inch (mm)	0.75 x 1.32 (19 x 33.5)	0.75 x 1.07 (19 x 27.2)
Case	material	St Stl	St Stl
Sealing		Epoxy	Epoxy
Weight	oz (gram)	3.1 (87)	1.9 (55)
Connector (micro)	coaxial	10-32	10-32
NOTES:			
[1] Zero Based Best Straight Line.			
[2] Mounted Resonance.			
[3] To achieve full range output, min. excitation voltage should be +21 VDC.			
SUPPLIED ACCESSORIES:			
Model 081B05 Mounting Stud			
Model 080A24 Petro Wax			
Model 085A01 RTV Boot (308B)			
Model 085A05 RTV Boot (308B03)			
APP'D	<i>Tm</i>	11-13-90	SPEC NO. 308-2010-80
ENGR	<i>ht</i>	11 13 90	
SALES	JAC	11-13-90	



PDV-100 Technical Data

General Specifications			
Decoder type	DSP velocity decoder, 3 measurement ranges		
Frequency range	0 ... 22 kHz (digital output); 0.5 Hz ... 22 kHz (analog output)		
Measurement ranges	3		
Full scale peak ¹⁾ (mm s ⁻¹)	20	100	500
Scaling factor (mm s ⁻¹ /V)	5	25	125
Velocity resolution ²⁾ (µm s ⁻¹ /√Hz)	< 0.02	< 0.02	< 0.1
Maximum acceleration (m s ⁻²)	2,760	13,800	69,000
Working distance ³⁾	0.1 m ... ca. 30 m		
Laser safety	Eye-safe class II visible HeNe laser		

¹⁾ Adjustable via the display.

²⁾ The resolution is defined as the signal amplitude (rms) at which the signal-to-noise ratio is 0 dB in a 1 Hz spectral bandwidth (RBW), measured on 3M Scotchlite[®] tape.

³⁾ The maximum stand-off distance depends on the surface properties of the object.

Output Signals	
Analog velocity output	
Output voltage swing	± 4 V (24 bit DAC)
Frequency range	0.5 Hz ... 22 kHz
Dynamic range ¹⁾	> 90 dB
Calibration accuracy	± 1 % (20 Hz ... 22 kHz)
Digital velocity output	
Electrical S/P-DIF interface ²⁾	24 bit, 48 kSa/s
Frequency range	0 ... 22 kHz
Calibration accuracy	± 0.2 % (0.05 Hz ... 22 kHz)
Output filter	
Digital low pass filter (FIR type)	1, 5, 22 kHz (-0.1 dB), roll-off >120 dB/dec
Analog high pass filter	100 Hz (-3 dB), roll-off -60 dB/dec

¹⁾ Defined as spurious free dynamic range (SFDR).

²⁾ S/P-DIF: Sony/Philips Digital Audio InterFace.

Housing and Power	
Dimensions L x W x H	300 mm x 63 mm x 129 mm (11.8 in x 2.5 in x 5.1 in)
Weight	~ 2.6 kg (~ 5.7 lbs)
Protection rating	IP 64 (dust and spray water protected)
Power	12 V DC, max. 15 W
Operating temperature	+5 °C ... +40 °C (41 °F ... 104 °F)
Storage temperature	-10 °C ... +65 °C (14 °F ... 149 °F)
Relative humidity	max. 80 %, non-condensing
Display	LCD, 3-line, with background lighting
Battery Kit PDV-BS	Rechargeable Li-Ion battery for min. 4 hours operation time

Compliance with Standards	
Electrical safety	IEC/EN61010
EMC	IEC/EN61326
Laser safety	IEC/EN60825-1



Polytec GmbH (Germany)
Polytec-Platz 1-7
76337 Waldbronn
Tel. + 49 (0) 7243 604-0
Fax + 49 (0) 7243 69944
info@polytec.de

Polytec-PI, S.A. (France)
32 rue Délizy
93694 Pantin
Tel. + 33 (0) 1 48 10 39 34
Fax + 33 (0) 1 48 10 09 66
info@polytec-pi.fr

Lambda Photometrics Ltd. (Great Britain)
Lambda House, Batford Mill
Harpenden, Herts AL5 5BZ
Tel. + 44 (0) 1582 764334
Fax + 44 (0) 1582 712084
info@lambdaphoto.co.uk

Polytec KK (Japan)
Hakusan High Tech Park
1-18-2 Hakusan, Midori-ku
Yokohama-shi, 226-0006
Kanagawa-ken
Tel. +81 (0) 45 938-4960
Fax +81 (0) 45 938-4961
info@polytec.co.jp

Polytec, Inc. (USA)
North American Headquarters
1342 Bell Avenue, Suite 3-A
Tustin, CA 92780
Tel. +1 714 850 1835
Fax +1 714 850 1831
info@polytec.com

Midwest Office
3915 Research Park Dr.
Suite A-12
Ann Arbor, MI 48108
Tel. +1 734 662 4900
Fax +1 734 662 4451

East Coast Office
25 South Street, Suite A
Hopkinton, MA 01748
Tel. +1 508 544 1224
Fax +1 508 544 1225

APPENDIX F

Structural Response Magnitudes

Table F.1: Vibration magnitudes measured in unweighted and W_k ms^{-2} weighted acceleration between 10 and 100 Hz. Values represent the response to a 1 Newton unit force impulse at each stage measurement position.

Measurement	ms^{-2}	$W_k \text{ms}^{-2}$
Slab-1, 1m, Front	2.736	0.42
Slab-1, 2m Front	2.165	0.301
Slab-1, 1m, Side	4.012	0.562
Slab-1, 2m, Side	1.166	0.157
Slab-1, 4m, Side	0.311	0.052
Slab-2, 1m, Front	5.455	0.978
Slab-2, 2m, Front	4.811	0.616
Slab-2, 4m, Front	1.406	0.171
Slab-2, 1m, Side	3.199	0.361
Slab-2, 2m, Side	1.305	0.135
Slab-2, 4m, Side	0.441	0.049
Joist-1, 1m, Front	0.175	0.026
Joist-1, 2m, Front	0.124	0.018
Joist-1, 4m, Front	0.078	0.011
Joist-1, 1m, Side	0.543	0.086
Joist-1, 2m, Side	0.313	0.069
Joist-1, 4m, Side	0.425	0.071
Pit Riser, 1m, Side	5.862	0.846
Pit Riser, 2m, Side	3.305	0.497
Pit Riser, 4m, Side	1.181	0.196
Joist-2, 1m, Front	3.679	0.727
Joist-2, 2m, Front	1.99	0.415
Joist-2, 4m, Front	0.532	0.117
Joist-2, 1m, Side	2.056	0.456
Joist-2, 2m, Side	1.518	0.241
Joist-2, 4m, Side	1.303	0.241

APPENDIX G

Structural Frequency Response Functions

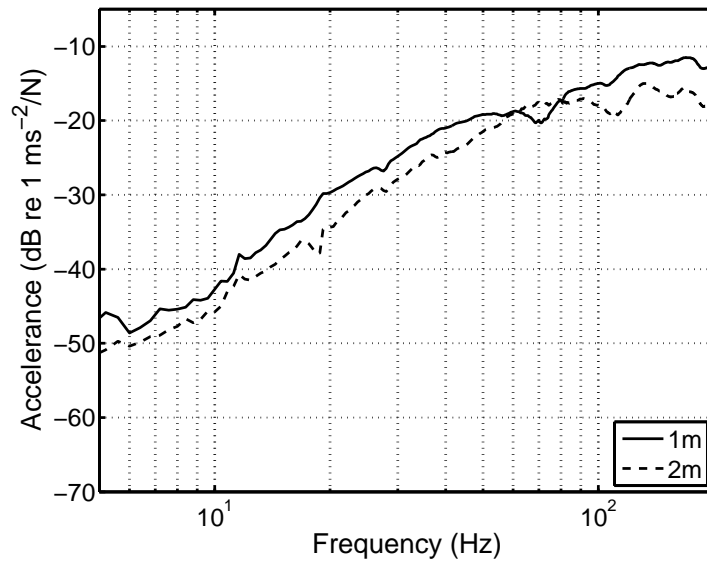


Figure G.1: Accelerance frequency response functions for Slab-A construction in the front direction.

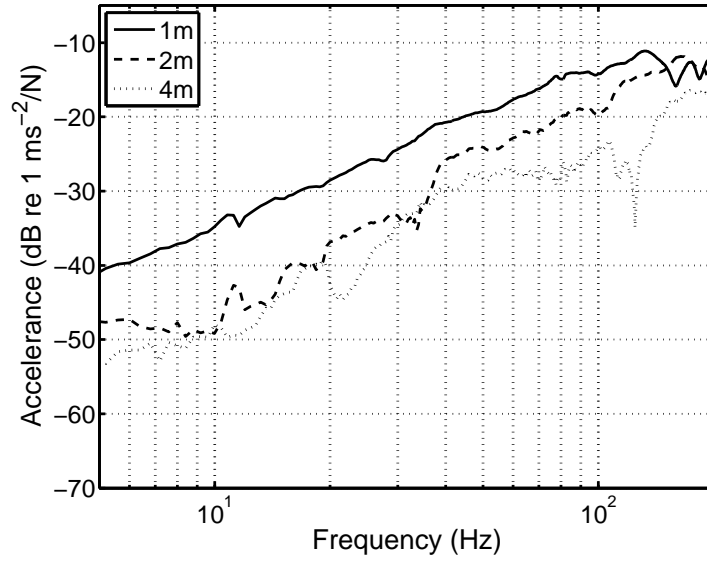


Figure G.2: Accelerance frequency response functions for Slab-A construction in the side direction.

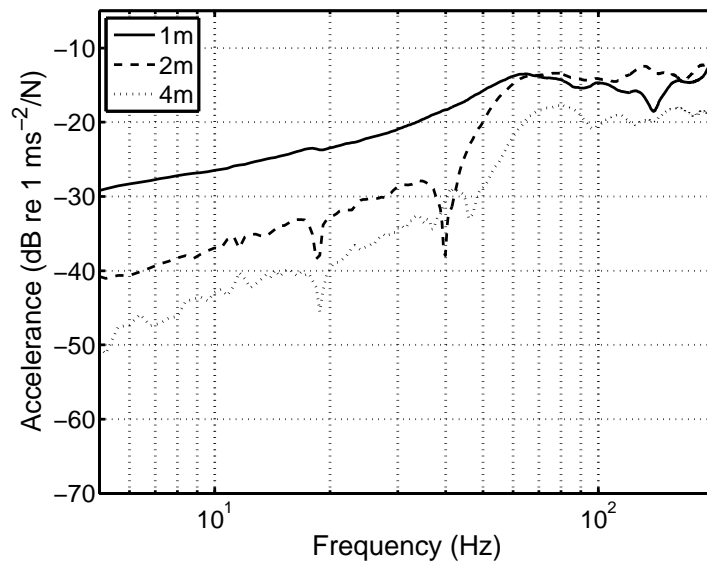


Figure G.3: Accelerance frequency response functions for Slab-B construction in the front direction.

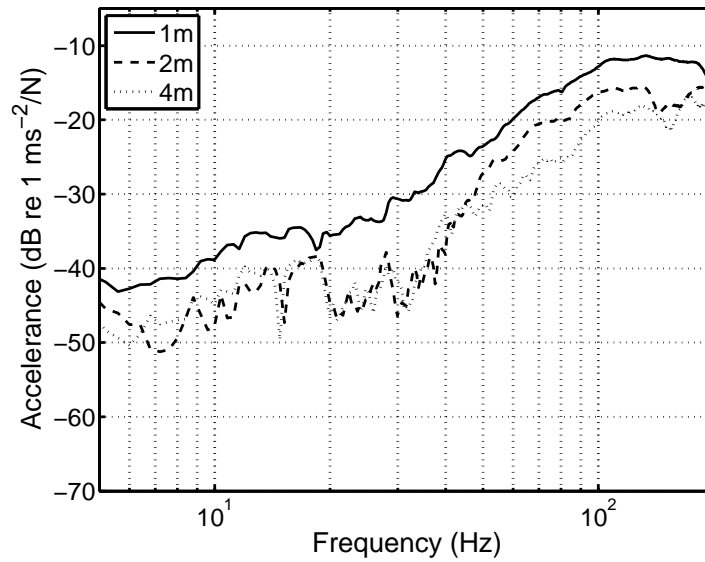


Figure G.4: Accelerance frequency response functions for Slab-B construction in the side direction.

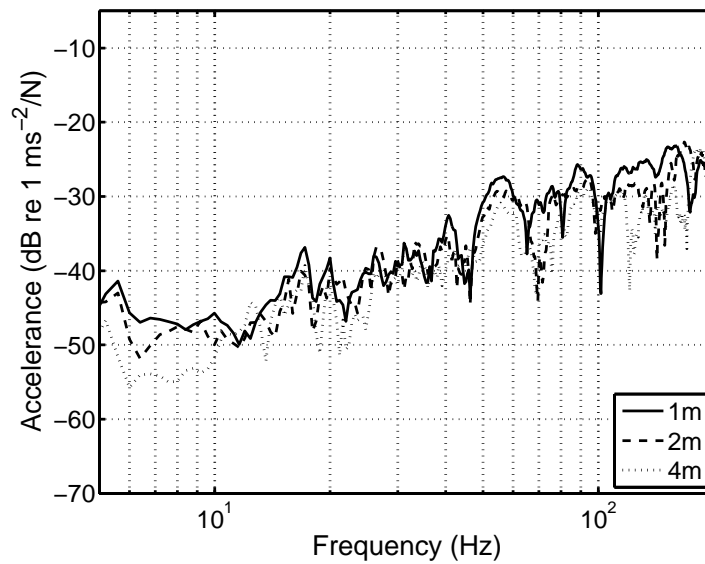


Figure G.5: Accelerance frequency response functions for Joist-A construction in the front direction.

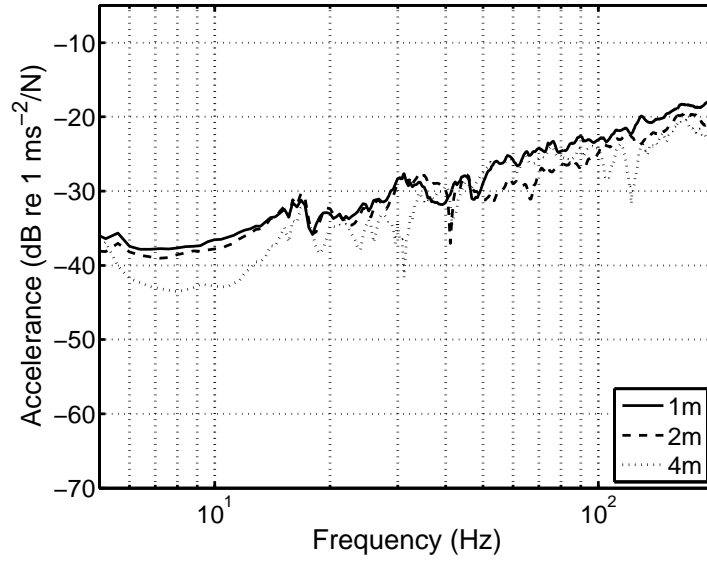


Figure G.6: Accelerance frequency response functions for Joist-A construction in the side direction.

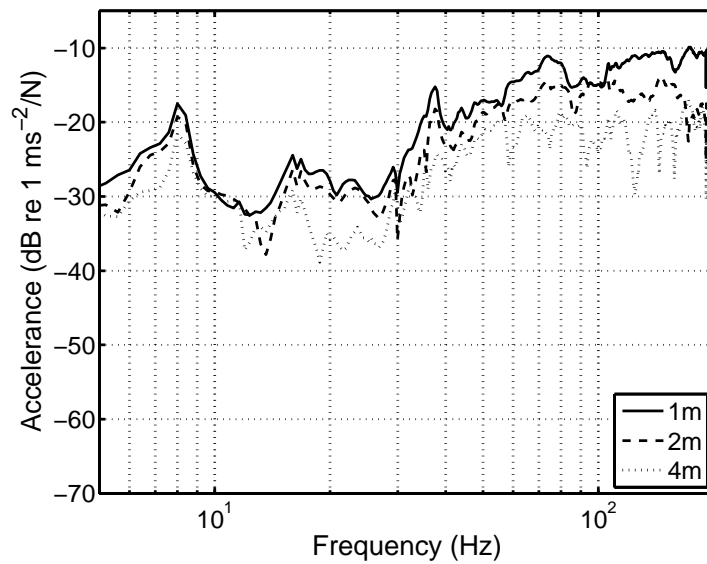


Figure G.7: Accelerance frequency response functions for Orchestra Pit Riser construction in the side direction.

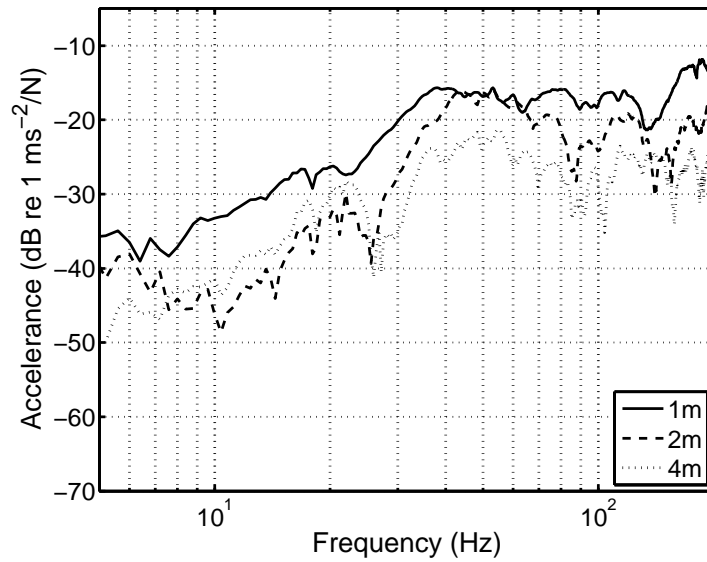


Figure G.8: Accelerance frequency response functions for Joist-B construction in the front direction.

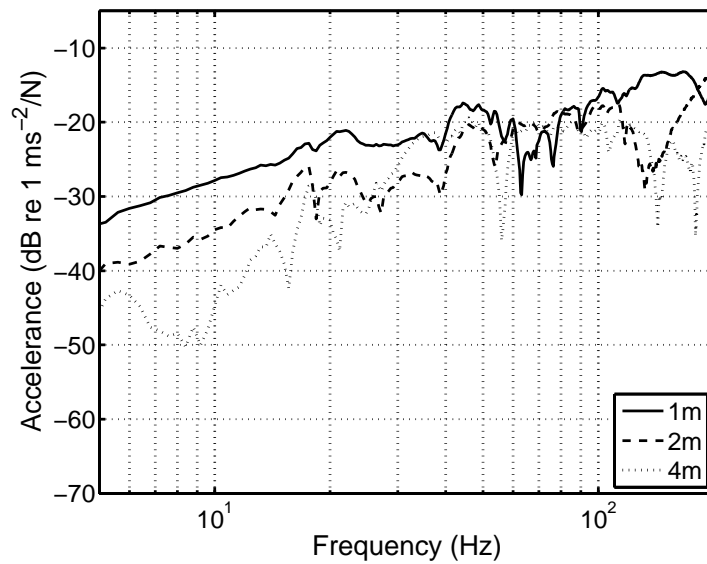


Figure G.9: Accelerance frequency response functions for Joist-B construction in the side direction.

APPENDIX H

Vibration Propagation Times

Table H.1: Vibration propagation times between source and receiver and time delays of vibration signal with respect to audio calculated using the cross-correlation function. Negative time delays indicate tactile lead.

Measurement	Prop. Time (ms)	Sound Speed (m/s)	Delay to Audio (ms)
Slab-1, 1m, Front	9	111.1	6.1
Slab-1, 2m Front	15.5	129	9.7
Slab-1, 1m, Side	7	142.9	4.1
Slab-1, 2m, Side	12.5	160	6.7
Slab-1, 4m, Side	16.5	242.4	4.9
Slab-2, 1m, Front	12.5	80	9.6
Slab-2, 2m, Front	13.5	148.1	7.7
Slab-2, 4m, Front	21.5	186	9.9
Slab-2, 1m, Side	9.5	105.3	6.6
Slab-2, 2m, Side	18.5	108.1	12.7
Slab-2, 4m, Side	31.5	127	19.9
Joist-1, 1m, Front	8	125	5.1
Joist-1, 2m, Front	29	69	23.2
Joist-1, 4m, Front	50.5	79.2	38.9
Joist-1, 1m, Side	3.5	285.7	0.6
Joist-1, 2m, Side	5.5	363.6	-0.3
Joist-1, 4m, Side	9	444.4	-2.6
Pit Riser, 1m, Side	16	62.5	13.1
Pit Riser, 2m, Side	37.5	53.3	31.7
Pit Riser, 4m, Side	58	69	46.4
Joist-2, 1m, Front	12.5	80	9.6
Joist-2, 2m, Front	32.5	61.5	26.7
Joist-2, 4m, Front	84	47.6	72.4
Joist-2, 1m, Side	5	200	2.1
Joist-2, 2m, Side	8	250	2.2
Joist-2, 4m, Side	15	266.7	3.4

APPENDIX I
Individual Subject Difference Matrices

Table I.1: Difference matrix: Subject #1

	1	2	3	4	5	6	7	8	9	10	11	12	13	14
1	0	3	2	1	3	1	2	5	1	2	4	2	2	6
2	3	0	4	5	6	4	5	6	4	5	2	2	3	5
3	2	4	0	4	3	1	2	3	3	1	5	4	6	7
4	1	5	4	0	6	5	5	6	3	4	4	1	3	3
5	3	6	3	6	0	2	2	3	6	5	6	6	6	6
6	1	4	1	5	2	0	1	3	4	3	6	5	6	7
7	2	5	2	5	2	1	0	3	1	1	5	4	3	7
8	5	6	3	6	3	3	3	0	3	3	7	6	6	7
9	1	4	3	3	6	4	1	3	0	1	4	3	4	6
10	2	5	1	4	5	3	1	3	1	0	3	4	5	6
11	4	2	5	4	6	6	5	7	4	3	0	1	2	2
12	2	2	4	1	6	5	4	6	3	4	1	0	3	6
13	2	3	6	3	6	6	3	6	4	5	2	3	0	5
14	6	5	7	3	6	7	7	7	6	6	2	6	5	0

Table I.2: Difference matrix: Subject #2

	1	2	3	4	5	6	7	8	9	10	11	12	13	14
1	0	5	3	4	5	3	2	3	3	2	5	2	5	7
2	5	0	5	4	5	6	6	7	3	1	4	7	4	4
3	3	5	0	7	3	1	4	1	4	2	6	5	5	7
4	4	4	7	0	6	6	3	7	2	4	7	3	5	4
5	5	5	3	6	0	3	2	2	2	3	5	6	5	7
6	3	6	1	6	3	0	1	3	3	2	7	6	6	7
7	2	6	4	3	2	1	0	2	4	4	6	4	5	6
8	3	7	1	7	2	3	2	0	6	5	7	5	5	7
9	3	3	4	2	2	3	4	6	0	3	4	1	3	7
10	2	1	2	4	3	2	4	5	3	0	6	3	4	5
11	5	4	6	7	5	7	6	7	4	6	0	6	5	4
12	2	7	5	3	6	6	4	5	1	3	6	0	2	4
13	5	4	5	5	5	6	5	5	3	4	5	2	0	5
14	7	4	7	4	7	7	6	7	7	5	4	4	5	0

Table I.3: Difference matrix: Subject #3

	1	2	3	4	5	6	7	8	9	10	11	12	13	14
1	0	2	3	4	4	5	2	6	3	1	3	1	4	5
2	2	0	4	1	5	4	4	7	2	2	2	1	2	3
3	3	4	0	4	1	1	3	3	3	3	4	4	3	6
4	4	1	4	0	4	2	4	2	2	2	5	1	3	2
5	4	5	1	4	0	1	2	2	4	5	6	4	6	5
6	5	4	1	2	1	0	2	1	2	3	6	5	6	7
7	2	4	3	4	2	2	0	4	1	3	6	4	6	6
8	6	7	3	2	2	1	4	0	5	4	5	5	5	7
9	3	2	3	2	4	2	1	5	0	2	3	3	3	5
10	1	2	3	2	5	3	3	4	2	0	4	2	2	4
11	3	2	4	5	6	6	6	5	3	4	0	2	2	2
12	1	1	4	1	4	5	4	5	3	2	2	0	2	3
13	4	2	3	3	6	6	6	5	3	2	2	2	0	3
14	5	3	6	2	5	7	6	7	5	4	2	3	3	0

Table I.4: Difference matrix: Subject #4

	1	2	3	4	5	6	7	8	9	10	11	12	13	14
1	0	3	4	3	4	2	3	4	2	4	6	2	3	5
2	3	0	2	2	6	4	5	6	2	4	3	2	2	1
3	4	2	0	4	4	2	1	3	2	2	6	3	5	7
4	3	2	4	0	3	5	5	6	4	3	3	3	2	4
5	4	6	4	3	0	2	1	1	3	1	6	6	5	7
6	2	4	2	5	2	0	1	2	2	2	5	5	5	6
7	3	5	1	5	1	1	0	3	3	2	4	4	4	6
8	4	6	3	6	1	2	3	0	4	5	5	5	5	6
9	2	2	2	4	3	2	3	4	0	2	2	3	3	6
10	4	4	2	3	1	2	2	5	2	0	5	4	3	4
11	6	3	6	3	6	5	4	5	2	5	0	1	2	2
12	2	2	3	3	6	5	4	5	3	4	1	0	2	2
13	3	2	5	2	5	5	4	5	3	3	2	2	0	3
14	5	1	7	4	7	6	6	6	6	4	2	2	3	0

Table I.5: Difference matrix: Subject #5

	1	2	3	4	5	6	7	8	9	10	11	12	13	14
1	0	2	1	1	2	1	2	2	1	1	5	2	2	5
2	2	0	4	2	6	3	5	5	2	4	1	1	1	3
3	1	4	0	3	5	2	1	2	1	2	5	3	4	6
4	1	2	3	0	5	2	5	3	4	4	4	2	3	5
5	2	6	5	5	0	1	2	2	3	3	7	5	6	6
6	1	3	2	2	1	0	1	1	2	2	5	2	4	7
7	2	5	1	5	2	1	0	4	3	3	5	3	3	7
8	2	5	2	3	2	1	4	0	4	5	6	5	6	6
9	1	2	1	4	3	2	3	4	0	2	4	2	3	6
10	1	4	2	4	3	2	3	5	2	0	2	3	4	7
11	5	1	5	4	7	5	5	6	4	2	0	4	3	3
12	2	1	3	2	5	2	3	5	2	3	4	0	2	2
13	2	1	4	3	6	4	3	6	3	4	3	2	0	3
14	5	3	6	5	6	7	7	6	6	7	3	2	3	0

Table I.6: Difference matrix: Subject #6

	1	2	3	4	5	6	7	8	9	10	11	12	13	14
1	0	2	3	2	6	2	4	6	4	2	2	2	5	3
2	2	0	5	3	5	5	6	3	1	5	3	5	5	4
3	3	5	0	3	2	3	1	4	6	3	6	5	5	3
4	2	3	3	0	5	3	3	7	2	4	2	2	1	5
5	6	5	2	5	0	2	4	3	5	1	7	4	5	5
6	2	5	3	3	2	0	2	2	1	2	2	5	5	2
7	4	6	1	3	4	2	0	4	3	1	4	3	5	5
8	6	3	4	7	3	2	4	0	4	2	5	4	4	6
9	4	1	6	2	5	1	3	4	0	4	1	2	3	4
10	2	5	3	4	1	2	1	2	4	0	3	2	1	4
11	2	3	6	2	7	2	4	5	1	3	0	4	3	3
12	2	5	5	2	4	5	3	4	2	2	4	0	1	4
13	5	5	5	1	5	5	5	4	3	1	3	1	0	2
14	3	4	3	5	5	2	5	6	4	4	3	4	2	0

Table I.7: Difference matrix: Subject #7

	1	2	3	4	5	6	7	8	9	10	11	12	13	14
1	0	4	3	3	2	1	1	3	2	4	4	4	6	6
2	4	0	4	3	5	5	6	6	1	3	4	3	2	3
3	3	4	0	6	2	2	4	3	3	5	4	3	7	7
4	3	3	6	0	5	2	5	6	3	3	5	2	3	3
5	2	5	2	5	0	2	1	3	6	5	6	6	5	6
6	1	5	2	2	2	0	1	4	1	2	7	6	5	6
7	1	6	4	5	1	1	0	1	3	4	6	5	7	7
8	3	6	3	6	3	4	1	0	4	5	6	6	7	7
9	2	1	3	3	6	1	3	4	0	2	4	4	3	6
10	4	3	5	3	5	2	4	5	2	0	3	1	2	4
11	4	4	4	5	6	7	6	6	4	3	0	4	3	1
12	4	3	3	2	6	6	5	6	4	1	4	0	2	5
13	6	2	7	3	5	5	7	7	3	2	3	2	0	5
14	6	3	7	3	6	6	7	7	6	4	1	5	5	0

Table I.8: Difference matrix: Subject #8

	1	2	3	4	5	6	7	8	9	10	11	12	13	14
1	0	5	1	3	1	2	4	6	1	1	5	4	3	5
2	5	0	4	1	5	5	6	7	3	4	2	2	1	3
3	1	4	0	6	4	1	1	4	1	2	5	5	7	6
4	3	1	6	0	7	5	3	7	2	4	3	1	3	2
5	1	5	4	7	0	3	2	2	3	4	7	5	7	7
6	2	5	1	5	3	0	3	3	1	3	6	5	7	6
7	4	6	1	3	2	3	0	2	5	2	5	6	7	7
8	6	7	4	7	2	3	2	0	5	3	7	6	7	7
9	1	3	1	2	3	1	5	5	0	2	4	1	3	6
10	1	4	2	4	4	3	2	3	2	0	2	1	1	4
11	5	2	5	3	7	6	5	7	4	2	0	2	4	3
12	4	2	5	1	5	5	6	6	1	1	2	0	2	3
13	3	1	7	3	7	7	7	7	3	1	4	2	0	2
14	5	3	6	2	7	6	7	7	6	4	3	3	2	0

Table I.9: Difference matrix: Subject #9

	1	2	3	4	5	6	7	8	9	10	11	12	13	14
1	0	5	1	4	4	3	2	3	1	5	4	3	6	6
2	5	0	5	5	7	3	4	5	5	3	2	3	2	4
3	1	5	0	5	2	2	1	3	2	2	7	5	6	6
4	4	5	5	0	5	6	3	6	3	4	5	3	4	5
5	4	7	2	5	0	2	1	1	5	2	5	5	4	7
6	3	3	2	6	2	0	1	1	2	2	6	2	7	7
7	2	4	1	3	1	1	0	2	3	2	5	4	6	7
8	3	5	3	6	1	1	2	0	6	3	6	6	5	7
9	1	5	2	3	5	2	3	6	0	2	6	3	6	7
10	5	3	2	4	2	2	2	3	2	0	6	3	6	6
11	4	2	7	5	5	6	5	6	6	6	0	2	5	3
12	3	3	5	3	5	2	4	6	3	3	2	0	3	5
13	6	2	6	4	4	7	6	5	6	6	5	3	0	5
14	6	4	6	5	7	7	7	7	7	6	3	5	5	0

Table I.10: Difference matrix: Subject #10

	1	2	3	4	5	6	7	8	9	10	11	12	13	14
1	0	2	2	5	5	3	1	4	5	3	5	2	7	5
2	2	0	2	5	4	4	7	5	4	7	5	2	3	5
3	2	2	0	5	2	4	1	2	1	5	5	3	3	7
4	5	5	5	0	4	5	2	4	4	3	7	2	5	6
5	5	4	2	4	0	5	4	3	5	3	7	4	6	7
6	3	4	4	5	5	0	3	6	3	3	6	4	6	5
7	1	7	1	2	4	3	0	2	2	2	6	3	4	7
8	4	5	2	4	3	6	2	0	5	4	6	5	7	7
9	5	4	1	4	5	3	2	5	0	3	4	6	4	7
10	3	7	5	3	3	3	2	4	3	0	3	3	6	6
11	5	5	5	7	7	6	6	6	4	3	0	4	4	1
12	2	2	3	2	4	4	3	5	6	3	4	0	3	6
13	7	3	3	5	6	6	4	7	4	6	4	3	0	4
14	5	5	7	6	7	5	7	7	7	6	1	6	4	0

APPENDIX J
Correlation Coefficients for MDS Configuration Axis and
Physical Parameters

Table J.1: Pearson product-moment correlation coefficients for correlation of physical parameters to two-way MDS configurations.

Space/ Dim.	$\%>$ thresh.	ms^{-2} r.m.s.	ms^{-2} r.m.q.	$W_k \text{ ms}^{-2}$ r.m.s.	$W_k \text{ ms}^{-2}$ r.m.q.	ms^{-1} r.m.s.	ms^{-1} r.m.q.	dT (ms)	B.R. 50Hz	B.R. 72Hz	Spec. CoG (Hz)
1D	-0.91	-0.95	-0.86	-0.91	-0.92	0.42	0.43	-0.02	0.58	0.4	-0.44
2D-1	0.92	0.95	0.84	0.91	0.92	-0.47	-0.48	0	-0.55	-0.39	0.42
2D-2	-0.13	0.02	-0.01	-0.14	-0.12	0.04	0.01	0.05	-0.47	-0.46	0.58
3D-1	0.91	0.94	0.84	0.91	0.91	-0.47	-0.48	-0.02	-0.57	-0.41	0.45
3D-2	-0.18	-0.03	-0.07	-0.19	-0.18	0.07	0.04	0.08	-0.36	-0.37	0.47
3D-3	0.16	-0.13	-0.33	0.14	0.09	0.02	0.02	0.48	0.07	0.31	-0.18

Table J.2: Pearson product-moment correlation coefficients for correlation of physical parameters to individual difference scaling MDS configurations.

Space/ Dim.	%> thresh.	ms^{-2} r.m.s.	ms^{-2} r.m.q.	$\mathbf{W}_k \text{ms}^{-2}$ r.m.s.	$\mathbf{W}_k \text{ms}^{-2}$ r.m.q.	ms^{-1} r.m.s.	ms^{-1} r.m.q.	dT (ms)	B.R. 50Hz	B.R. 72Hz	Spec. CoG (Hz)
1D	0.92	0.95	0.84	0.92	0.92	-0.44	-0.44	0.02	-0.51	-0.36	0.38
2D-1	0.76	0.83	0.72	0.75	0.75	-0.38	-0.4	0.05	-0.66	-0.53	0.59
2D-2	0.87	0.81	0.74	0.87	0.87	-0.44	-0.43	-0.04	-0.2	-0.04	0.01
3D-1	0.93	0.92	0.85	0.93	0.93	-0.47	-0.47	-0.09	-0.49	-0.32	0.33
3D-2	0.53	0.58	0.43	0.51	0.51	-0.31	-0.33	0.21	-0.48	-0.37	0.45
3D-3	-0.16	0.12	0.27	-0.14	-0.11	0	0	-0.42	-0.1	-0.41	0.28